
ORDER, DISORDER, AND PHASE TRANSITION
IN CONDENSED SYSTEM

Quantum Renormalizations in Anisotropic Multisublattice Magnets and the Modification of Magnetic Susceptibility under Irradiation

V. V. Val'kov^a and M. S. Shustin^{a,b}

^a Kirenskii Institute of Physics, Siberian Branch, Russian Academy of Sciences, Akademgorodok, Krasnoyarsk, 660036 Russia

^b Siberian Federal University, Krasnoyarsk, 660041 Russia

e-mail: vvv@iph.krasn.ru

Received May 29, 2015

Abstract—The dispersion equation of a strongly anisotropic one-dimensional magnet catena-[Fe^{II}(ClO₄)₂{Fe^{III}(bpca)₂}]ClO₄ containing alternating high-spin (HS) ($S = 2$) and low-spin (LS) ($S = 1/2$) iron ions is obtained by the diagram technique for Hubbard operators. The analysis of this equation yields six branches in the excitation spectrum of this magnet. It is important that the crystal field for ions with spin $S = 2$ is described by the Hamiltonian of single-ion easy-plane anisotropy, whose orientation is changed by 90° when passing from one HS iron ion to another. The $U(N)$ transformation technique in the atomic representation is applied to diagonalize a single-ion Hamiltonian with a large number of levels. It is shown that the modulation of the orientation of easy magnetization planes leads to a model of a ferrimagnet with easy-axis anisotropy and to the formation of energy spectrum with a large gap. For HS iron ions, a decrease in the mean value of the spin projection due to quantum fluctuations is calculated. The analysis of the specific features of the spectrum of elementary excitations allows one to establish a correspondence to a generalized Ising model for which the magnetic susceptibility is calculated in a wide range of temperatures by the transfer-matrix method. The introduction of a statistical ensemble that takes into account the presence of chains of different lengths and the presence of iron ions with different spins allows one to describe the experimentally observed modification of the magnetic susceptibility of the magnet under optical irradiation.

DOI: 10.1134/S1063776115110175

1. INTRODUCTION

The analysis of the specific features of magnetic ordering and phases in quantum spin chains has been attracting great interest of researchers in view of significant manifestation of quantum fluctuations in these systems [1–4]. Recent progress in the field of synthesis of organic magnetic compounds [5] has opened a possibility for a detailed experimental investigation of low-dimensional magnetic structures, including single-chain magnets (SCMs). To date, a few tens of materials of this class have been synthesized that demonstrate a large variety of physical properties [6, 7]. The common property of these compounds is the presence of organic ligands that are responsible for the screening of magnetic interactions between individual chains and induce strong single-ion anisotropy. In most cases, this anisotropy is of easy-axis type. Therefore, at finite temperatures, single-chain magnets have no long-range magnetic order, and their ground state represents a set of ordered domains. Such domains are characterized by the correlation length ζ , which can reach values of $\zeta \sim 10^2\text{--}10^4$ Å in real SCM compounds at temperatures of $T \sim 1$ K. Due to the strong anisotropy, these domains are also characterized by a sharp (on the order of tens of angstrom) domain wall and

have excitation energy close to the exchange integral J between nearest neighbor ions belonging to the same chain. In this situation, the magnetic relaxation time in the system is determined by the characteristic time of “decay” of a domain through “wandering” of a domain wall in the chain. As shown in [6], the temperature dependence of this time at low temperatures exhibits exponential behavior: $\tau \propto \exp(\Delta/T)$, where Δ is the characteristic energy of a flip of a spin. Thus, one of characteristic features of SCMs is associated with the fact that, as temperature decreases, the magnetic relaxation time τ of the system increases exponentially and may reach values of about an hour at $T \sim 1$ K [8]. In view of the microscopic scale of magnetic domains and the slow dynamics of their magnetization, SCMs are currently not only of interest from the fundamental point of view [9], but are also considered as promising materials for the design of hardware components for memory devices.

Important information on the character of magnetic interactions in SCMs is provided by the behavior of the temperature dependence of the correlation length $\zeta(T)$ and the relaxation time $\tau(T)$. In the experimental investigations of SCM compounds, these characteristics are usually derived from the measure-

ments of the temperature dependence of the static $\chi(T)$ and dynamic $\chi(\omega, T)$ magnetic susceptibilities by the formulas $\chi(T) \sim \zeta/T$ and $\chi(\omega, T) \sim \chi/(1 - i\omega\tau)$. Hence, a purposeful study of the magnetic properties of SCMs can be carried out on the basis of the analysis of static and dynamic characteristics [6].

To describe the static magnetic properties of SCMs, most often one applies either generalizations of the Ising model or the classical Heisenberg model in which the vector operators of spin moments \mathbf{S} are replaced by classical vectors. When studying the dynamic behavior of SCMs, one uses the generalizations of the Glauber model [10]. The latter is a kinetic version of the Ising model in which a random flip of a spin is modeled by phenomenological introduction of interaction between an Ising chain and a thermal reservoir. In these models, the operator nature of spins is neglected, and the applicability of such an approximation to the description of the physical properties of SCMs is argued by the presence of a strong uniaxial anisotropy in the system, as well as by relatively large values of spins of magnetically active ions. For a more accurate representation of real features of SCMs, the above-mentioned models were analyzed in detail and extended to the cases of the presence in the systems of nonmagnetic impurities [11–44], ferrimagnetism [15], strong magnetic fields [16], mutual noncollinearity of anisotropy axes [17, 18], and isotropic quantum moments [19].

In recent years, an important field of research has been associated with the study of the prospects of designing SCMs that would demonstrate not only slow dynamics, but also the presence of spin crossovers [8, 21–24], as well as photoinduced states [8, 25–27]. Of special interest are SCMs whose magnetic properties can be changed under external irradiation [8, 25]. It is believed that the states of the magnetic subsystem in these compounds can be changed by a photoinduced modification of the states of the electron subsystem. Since the characteristic times of the dynamics of the magnetic subsystem in these compounds are much greater than the characteristic times of the dynamics of the electron subsystem, this feature allows one to consider SCMs not only as promising components for super high-density magnetic recording but also as components of superfast magnetic switches [28]. An increase in the number of possible applications of SCMs is associated, first of all, with progress in the field of synthesis of these compounds [7]. It is important that, among synthesized SCMs, there are compounds in which quantum effects play a significant role. These compounds also exhibit slow dynamics of magnetization, which, however, cannot be described within the Glauber model [7]. The formulation of theoretical models for describing most such compounds presents a separate problem.

One of the most interesting magnets from the viewpoint of the magnetic structure and the diversity of

physical properties is the single-chain magnet catena-[Fe^{II}(ClO₄)₂{Fe^{III}(bpca)₂}]ClO₄ (in what follows, SCM-catena) [6, 7, 27, 29–31] (Fig. 1). Experimental investigations of SCM-catena show that its magnetic susceptibility $\chi(T)$ exhibits strong variation under external irradiation [27]. The interpretation of this phenomenon is based on the assumption of a photoinduced change in the magnetic state of the system due to metal-to-metal charge transfer (MMCT) (Fig. 2) [27]. It was assumed that each quantum of radiation absorbed by the system induces an electron transition from the electron shell of high-spin (HS) state of Fe^{II} ($S = 2$) ion to the electron shell of Fe^{III} ion, which is in a low-spin (LS) state $S = 1/2$. In this case, the first iron ion finds itself in a state with $S = 5/2$, and the second iron ion, in a state with $S = 0$ (Fig. 2). The appearance of iron ions in a nonmagnetic state implies the breaking of exchange bonds and the formation of finite spin chains of various lengths. The theoretical description of the system is largely complicated by the specific features of the magnetic structure of the compound: the magnetic states of HS ions are formed with the participation of strong single-ion easy-plane anisotropy, whose orientation is changed when passing from one HS iron ion to another (Fig. 1). As a result of such a modulation, the compound displays properties characteristic of magnets with easy-axis anisotropy [30]. However, due to the presence of strong single-ion anisotropy, the compound should exhibit quantum fluctuations [33–36]. In particular, it is known that SCM-catena demonstrates slow dynamics of magnetization $\tau \propto \exp(\Delta/T)$ at low temperatures, which is characteristic of uniaxial one-dimensional magnets; however, the value of Δ significantly differs from the value predicted by the Glauber model; the authors of [30] attribute this fact to the presence of easy-magnetization planes in the compound.

In the present study, we apply the diagram technique for Hubbard operators [32, 37, 38], which allows us to rigorously describe anisotropic systems with arbitrary nonequidistance of single-ion energy levels. We also calculate the spectrum of magnetic excitations and the low-temperature thermodynamics of four-sublattice SCM-catena with regard to the fact that easy-magnetization planes of two neighboring HS iron ions have different orientations. We show that the different orientation of these easy-magnetization planes leads to the excitation spectrum that almost coincides with the excitation spectrum of an easy-axis ferrimagnet whose effective anisotropy parameter is comparable with the exchange integral. In both cases, the gap in the excitation spectrum is greater than the width of the spin-wave band. This means that the Ising model is implemented in the magnet. It turns out that spin fluctuations manifest themselves in that, in the ground state of the system, the mean value of the z -projection of the spin of an ion in the HS state with $S = 2$ decreases to a value of $\langle S^z \rangle \approx 3/2$. These results have

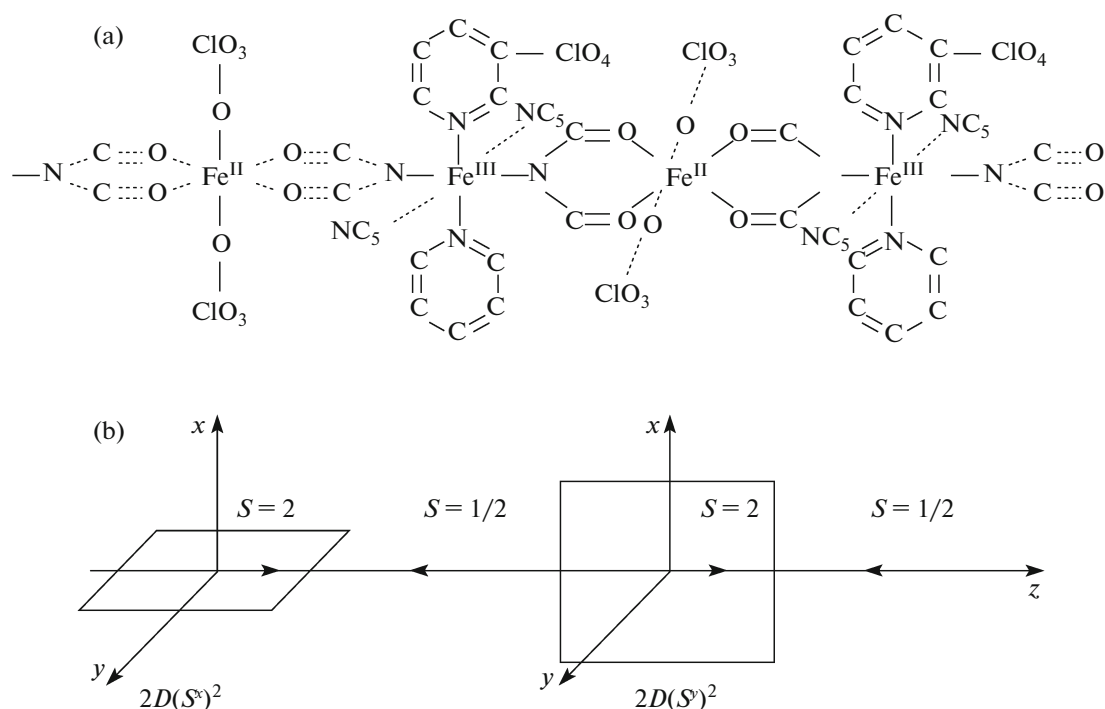


Fig. 1. (a) A fragment of the structure of single-chain magnet SCM-catena and (b) four-sublattice ferrimagnetic order in the strongly anisotropic one-dimensional magnet SCM-catena at temperatures $T < 7$ K. The figure illustrates a change in the orientation of easy-magnetization planes for nearest neighbor HS ions of iron. The following sequence of notations is introduced for sublattices: $A-B-C-D$ [29].

allowed us to consider the SCM-catena magnet within a spin-chain model with alternating pseudospin moments $\tilde{S} = 3/2$ and $\sigma = 1/2$ between which the

Ising-type exchange interaction occurs. This analogy allows one to apply the transfer-matrix method to calculate exact thermodynamic functions. In particular, taking into account the specific features of the ligand environment of iron ions in SCM-catena and a change in their charge distribution due to irradiation allow one to explain the experimentally observed anomalously strong variation in the magnetic susceptibility of SCM-catena. The appearance of iron ions in different charge and spin states, as well as the appearance of finite spin chains of different lengths, requires the introduction of a large statistical ensemble. Such an approach can be successfully applied to describe the experimentally observed modification of the temperature dependence of magnetic susceptibility under irradiation in other SCMs as well [8, 25, 26].

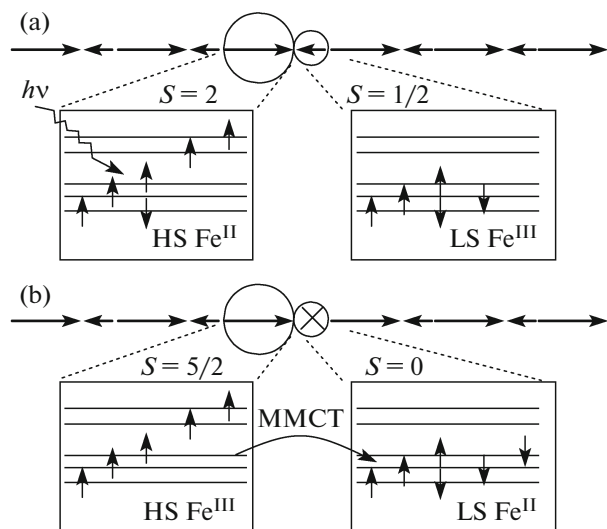


Fig. 2. A change in the spin configuration of HS and LS iron ions in SCM-catena during a photoinduced MMCT process [27]. The upper row demonstrates the electron configurations corresponding to HS and LS iron ions before irradiation. The lower row demonstrates that, after irradiation, when an electron is removed from an HS iron ion and an electron is added to an LS iron ion, two ions arise with spins $S = 5/2$ and 0, respectively.

2. SPIN HAMILTONIAN OF SCM-CATENA

In quasi-one-dimensional magnet catena- $[\text{Fe}^{\text{II}}(\text{ClO}_4)_2\{\text{Fe}^{\text{III}}(\text{bpca})_2\}]\text{ClO}_4$ [29], magnetically active iron ions are alternatively in states with different valences (Fig. 1b). Fe^{II} ions are surrounded by oxygen ions, which form a distorted octahedron. For d electrons in these ions, the case of a weak crystal field is implemented, and the configuration d^6 corresponds to the HS state with $S = 2$. According to HF-EPR spectroscopy data, the distortion of the ligand environ-

ment of Fe^{II} ions leads to the formation of easy-plane-type single-ion anisotropy [29].

Fe^{III} ions are surrounded by nitrogen ions, which have a large charge compared to oxygen ions. As a result, the d^5 electron shell of Fe^{III} ions is in a strong crystal field. The main ion term corresponds to the LS state with $S = 1/2$ (Figs. 1, 2).

In what follows, it is important that the easy-magnetization planes of two nearest HS ions of iron are orthogonal with respect to each other (Fig. 1). Below we will show that such alternation induces an effective axis of easy magnetization directed along the chain (the z axis in Fig. 1). The existence of this axis was verified by experimental measurements of the field dependence of magnetization. It was established that, when a field is applied perpendicular to the chains, the magnetization increases relatively slowly and does not reach saturation up to magnetic fields of 50 kOe. When the magnetic field is applied along the chains, the magnetization reaches saturation even in a field of $H = 500$ Oe. The authors of [30] attributed such a strong anisotropy of the magnetic properties of the system to the above-mentioned effective easy-magnetization axis.

The second experimental result is the observation of a short-range magnetic order at temperatures of $T < 7$ K [30]. The measurements were carried out by the Mössbauer spectroscopy method. On the basis of the results of these measurements, as well as of the measurements of the dynamic magnetic susceptibility, the authors established that the relaxation time of the magnetic moment increases exponentially as temperature decreases and, for $T = 1$ K, reaches a value of about a minute. From the combination of these facts, the authors of [30] drew a conclusion that a magnetic state with dominant Ising-type exchange interaction is implemented in the system. It turns out that the temperature dependence of the relaxation time cannot be described within the classical Glauber model. This points to the fact that quantum fluctuations associated with the presence of easy-magnetization planes develop in the system [30, 33]. Therefore, it seems to be necessary to take into account quantum phenomena in the four-sublattice one-dimensional magnet catena- $[\text{Fe}^{\text{II}}(\text{ClO}_4)_2\{\text{Fe}^{\text{III}}(\text{bpc})_2\}]\text{ClO}_4$ with alternating HS and LS iron ions and with easy-plane anisotropy modulated along the direction and analyze the low-temperature excitation spectrum in order to correctly pass to an effective Ising-type model and analyze the thermodynamic properties.

We will carry out the quantum analysis of a system of aliovalent iron ions in SCM-catena within the Heisenberg model with regard to an easy-plane-type single-ion anisotropy operator that is inhomogeneous with respect to sites [29, 30]:

$$\begin{aligned} \hat{\mathcal{H}}_G = & J \sum_f [\mathbf{S}_{f,A} \mathbf{S}_{f,B} + \mathbf{S}_{f,B} \mathbf{S}_{f,C} + \mathbf{S}_{f,C} \mathbf{S}_{f,D} \\ & + \mathbf{S}_{f,D} \mathbf{S}_{f+1,A}] + 2D \sum_f [(S_{f,A}^x)^2 + (S_{f,C}^y)^2] \quad (1) \\ & - H \sum_f [g_1(S_{f,A}^z + S_{f,C}^z) + g_2(S_{f,B}^z + S_{f,D}^z)], \end{aligned}$$

where $\mathbf{S}_{f,A}$ and $\mathbf{S}_{f,C}$ are vector operators of the spin moments of iron ions in HS states ($S = 2$) belonging to a magnetic cell with number f (the cell contains four magnetic ions) and situated in positions A and C . These ions are in the crystal field, which is effectively described by the operator of easy-plane single-ion anisotropy. The intensity of the anisotropy is determined by the parameter D . For iron ions in positions A , the easy-magnetization plane is the plane yz , whereas, for iron ions in positions C , this is the plane xz ; $\mathbf{S}_{f,B}$ and $\mathbf{S}_{f,D}$ are vector operators of the spin moments of iron ions in the LS state $S = 1/2$ situated in positions B and D ; H is the external magnetic field in energy units; g_1 and g_2 are the g factors for HS and LS ions, respectively; and J is the exchange integral between nearest neighbor ions. The calculations performed in [29, 30] have shown that $J = 20$ and $D = 7$ K.

When calculating the low-temperature spectral properties of SCM-catena, we take into consideration that, for $T < 7$ K, the experimentally observed short-range ferrimagnetic order is implemented in the compound. Assume that the spontaneous magnetization of all ions is directed along the z axis. Introducing a self-consistent field (SCF) in a standard way, we express the Hamiltonian of the system as

$$\begin{aligned} \hat{\mathcal{H}}_G = & \sum_{f_1 \in A} \hat{\mathcal{H}}_{0,A}(f_1) + \sum_{f_2 \in B} \hat{\mathcal{H}}_{0,B}(f_2) \quad (2) \\ & + \sum_{f_3 \in C} \hat{\mathcal{H}}_{0,C}(f_3) + \sum_{f_4 \in D} \hat{\mathcal{H}}_{0,D}(f_4) + \hat{\mathcal{H}}_{\text{int}}, \end{aligned}$$

where single-site operators for the four sublattices are given by

$$\begin{aligned} \hat{\mathcal{H}}_{0,A}(f_1) &= 2D(S_{f_1}^x)^2 - h_1^- S_{f_1}^z, \\ \hat{\mathcal{H}}_{0,B}(f_2) &= -h_2^- S_{f_2}^z, \\ \hat{\mathcal{H}}_{0,C}(f_3) &= 2D(S_{f_3}^y)^2 - h_1^- S_{f_3}^z, \\ \hat{\mathcal{H}}_{0,D}(f_4) &= -h_2^- S_{f_4}^z, \\ h_1^- &= g_1 H + 2J\sigma, \\ h_2^- &= g_2 H - 2JM. \end{aligned} \quad (3)$$

In formulas (3), we introduced the following notations for the magnetic order shown in Fig. 1: $M = \langle S_{f,A} \rangle = \langle S_{f,C} \rangle$ and $\sigma = -\langle S_{f,B} \rangle = -\langle S_{f,D} \rangle$.

The interaction operator $\hat{\mathcal{H}}_{\text{int}}$ in (2) describes intersite correlations induced by the exchange interaction. The introduction of circular spin operators and the three-component vector $\mathbf{u} = \{S^z; S^+; S^-\}$ allows us to express the correlation term in a compact form:

$$\hat{\mathcal{H}}_{\text{int}} = \sum_{i=1}^{i=4} \sum_{\langle f_i f_{i+1} \rangle} (\Delta \mathbf{u}_{f_i}, \hat{V} \cdot \Delta \mathbf{u}_{f_{i+1}}), \quad (4)$$

$$\mathbf{u}_{f_s} \equiv \mathbf{u}_{f_i},$$

where $\Delta \mathbf{u} = \mathbf{u} - \langle \mathbf{u} \rangle$. The angle brackets under the sign of sum imply that the summation is performed over the nearest neighbor ions of the sublattices. When considering isotropic exchange interaction, the matrix \hat{V} can be represented as follows:

$$\hat{V}(f_i, f_{i+1}) = J(f_i, f_{i+1}) \begin{pmatrix} 1 & 0 & 0 \\ 0 & 0 & 1/2 \\ 0 & 1/2 & 0 \end{pmatrix}, \quad (5)$$

where $J(f_i, f_{i+1})$ is the integral of exchange interaction between iron ions belonging to sublattices f_i and f_{i+1} .

To determine the spectral properties of the system, we invoke the concept of the atomic representation, which allows us to correctly consider strong single-ion anisotropy [32, 33]. The introduction of the atomic representation suggests the diagonalization of the single-site terms of Hamiltonian (1). Due to the presence of alternating HS and LS states of iron ions, we carry out the diagonalization of the corresponding terms in (3) separately.

3. DIAGONALIZATION OF SINGLE-SITE TERMS OF THE HAMILTONIAN. INTRODUCTION OF THE ATOMIC REPRESENTATION

Consider iron ions in HS states that are subjected to easy-plane-type single-ion anisotropy. Introduce the Hubbard operators $X^{pq} = |p\rangle\langle q|$ ($p, q = 1, \dots, 5$) [32, 37] constructed on the complete basis $|p\rangle$ of eigenstates of the operators S_A^z and S_C^z of iron ions located in positions A and C , respectively. Then, omitting the indices of sites in the spin operators for a while, we can represent the Hamiltonian describing the HS states of iron ions in the unified form:

$$\hat{\mathcal{H}}_{HS} = 2D + \hat{\mathcal{H}}_{HS}^{(2)} + \hat{\mathcal{H}}_{HS}^{(3)}, \quad (6)$$

where

$$\hat{\mathcal{H}}_{HS}^{(2)} = -(\bar{h}_1 - 3D)X^{22} + (\bar{h}_1 + 3D)X^{44} + 3D(e^{2i\phi}X^{24} + e^{-2i\phi}X^{42}), \quad (7)$$

$$\hat{\mathcal{H}}_{HS}^{(3)} = -2\bar{h}_1(X^{11} - X^{55}) + 4DX^{33} + \sqrt{6}D(e^{2i\delta\phi}(X^{13} + X^{35}) + e^{-2i\phi}(X^{31} + X^{53})). \quad (8)$$

For $\phi = 0$, formulas (6)–(8) describe HS ions with the easy-magnetization plane yz , whereas $\phi = \pi/2$ corresponds to HS ions for which the easy-magnetization plane is xz . It follows from the above formulas that the operator structure of the single-site Hamiltonian is decomposed into quasi-two-level, $\hat{\mathcal{H}}_{HS}^{(2)}$, and quasi-three-level, $\hat{\mathcal{H}}_{HS}^{(3)}$, forms. This fact simplifies the diagonalization of the Hamiltonian as a whole, because each such form is independently reduced to the diagonal form. Here one should take into account that the diagonalization should be performed simultaneously with the self-consistent determination of the effective field \bar{h}_1 . It is convenient to solve such a problem by the method of transformations of the group $U(N)$ [35].

Introduce a set of unitary operators

$$U_{nm}(\alpha) = e^{(\alpha X^{nm} - \alpha^* X^{mn})} = 1 - (1 - \cos|\alpha|) \times (X^{nn} + X^{mm}) + \sin|\alpha|(e^{i\mu}X^{nm} + \text{H.c.}), \quad (9)$$

where $\alpha = |\alpha|e^{i\mu}$ is a parameter of unitary transformation. Then, defining the transformation laws of Hubbard operators under unitary rotations (9),

$$X^{pq} \rightarrow X^{pq}(\alpha) = U_{nm}(\alpha)X^{pq}U_{nm}^+(\alpha),$$

and performing the sequence of rotations

$$U(\xi) = U(\alpha, \beta, \gamma, \Omega) = U_{24}(\Omega)U_{53}(\gamma)U_{13}(\beta)U_{15}(\alpha) \quad (10)$$

with additionally introduced parameters of the transformation $\beta = |\beta|e^{i\nu}$, $\gamma = |\gamma|e^{i\delta}$, and $\Omega = |\Omega|e^{i\kappa}$, we can represent Hamiltonian (6) as

$$\hat{\mathcal{H}}_{HS} \rightarrow \hat{\mathcal{H}}_{HS}(\xi) = U(\xi)\hat{\mathcal{H}}_{HS}U^+(\xi) = \sum_{p=1}^5 E_p X^{pp}. \quad (11)$$

Here, ξ stands for the set of parameters $\xi = \{\alpha, \beta, \gamma, \Omega\}$. The conditions of vanishing of the off-diagonal matrix elements of the transformed Hamiltonian define a system of equations for the parameters of unitary transformations α, β, γ , and Ω , as well as the eigenvalues E_p and the eigenstates $|\psi_p\rangle = U(\xi, \phi)|p\rangle$ of the operator $\hat{\mathcal{H}}_{HS}$. In (11) and below, by the operators $X^{pq} = |\psi_p\rangle\langle\psi_q|$ are meant the Hubbard operators constructed on the eigenstates $|\psi_p\rangle$. Using the results of [35], we obtain

$$E_1 = 2D - \bar{h}_1 \cos 2\alpha - \{(2D + \bar{h}_1 \cos 2\alpha)^2 + 6D^2(1 + \sin 2\alpha)\}^{1/2},$$

$$E_{2,4} = 3D \mp (\bar{h}_1^2 + 9D^2)^{1/2}, \quad (12)$$

$$E_{3,5} = \frac{1}{2}(\varepsilon_3'' + \varepsilon_5'') \mp ((\varepsilon_3'' - \varepsilon_5'')^2 + \tilde{V}^2)^{1/2},$$

$$|\psi_1\rangle = \cos \alpha \cos |\beta| |1\rangle + e^{-i\nu} \sin |\beta| |3\rangle + \sin \alpha \cos |\beta| |5\rangle,$$

$$|\psi_2\rangle = \cos |\Omega| |2\rangle + e^{-i\kappa} \sin |\Omega| |4\rangle,$$

$$|\psi_3\rangle = -(e^{i\nu} \cos \alpha \sin |\beta| \cos |\gamma|$$

$$\begin{aligned}
 & +e^{-i\delta} \sin \alpha \sin |\gamma| |1\rangle + \cos |\beta| \cos |\gamma| |3\rangle \\
 & -(e^{i\nu} \sin \alpha \sin |\beta| \cos |\gamma| - e^{-i\delta} \cos \alpha \sin |\gamma| |5\rangle, \\
 & |\psi_5\rangle = (e^{i(\delta+\nu)} \cos \alpha \sin |\beta| \sin |\gamma| \\
 & - \sin \alpha \cos |\gamma| |1\rangle - e^{i\delta} \cos |\beta| \sin |\gamma| |3\rangle \\
 & +(e^{i(\delta+\nu)} \sin \alpha \sin |\beta| \sin |\gamma| + \cos \alpha \cos |\gamma| |5\rangle),
 \end{aligned} \tag{13}$$

where

$$\begin{aligned}
 \varepsilon_3'' &= 2D - \bar{h}_1 \cos 2\alpha + (2D - \bar{h}_1 \cos 2\alpha) f_{\pm}(\alpha) \\
 & - \sqrt{6D(\cos \alpha + \sin \alpha) \sin 2|\beta| \sqrt{1 - f_{\pm}^2(\alpha)}}, \\
 \varepsilon_5'' &= 2\bar{h}_1 \cos 2\alpha,
 \end{aligned}$$

$$\tilde{V} = \sqrt{6D(\cos \alpha - \sin \alpha) f_{\pm}(\alpha) - 2\bar{h}_1 \sin 2\alpha \sqrt{1 - f_{\pm}^2(\alpha)}}, \tag{14}$$

where we assumed that the parameter α of the unitary transformation is real. The phases ν , δ , and κ of three other complex parameters β , γ , and Ω appearing in (13) take different values depending on the type of HS ions of iron:

$$\begin{aligned}
 \nu = \delta = \kappa = 0; \quad \phi = 0, \\
 \nu = \delta = \kappa = \pi; \quad \phi = \pi/2
 \end{aligned} \tag{15}$$

for the easy-magnetization planes yz and xz , respectively. The moduli of the transformation parameters α and β are determined from the relations

$$\begin{aligned}
 & (f_{\pm}(\alpha) - 1)(\cos \alpha - \sin \alpha) \cos 2\alpha \\
 & + f_{\pm}(\alpha)(\cos \alpha + \sin \alpha) \sin 2\alpha \\
 & + \sqrt{2/3(1 - f_{\pm}^2(\alpha))} \sin 4\alpha = 0,
 \end{aligned} \tag{16}$$

$$\cos 2|\beta| = f_{\pm}(\alpha) = \frac{A(A+B) \pm \sqrt{2B(A-B)}}{(A+B)^2 + 1}, \tag{17}$$

where

$$\begin{aligned}
 A(\alpha) &= \frac{\sqrt{6}}{4} (\cos \alpha - \sin \alpha) \cot 2\alpha, \\
 B(\alpha) &= \frac{\sqrt{6}}{2} (\cos \alpha + \sin \alpha).
 \end{aligned}$$

The modulus of the parameter γ is determined by the formulas

$$\begin{aligned}
 \sin 2|\gamma| &= \frac{\varepsilon_3'' - \varepsilon_5''}{\sqrt{(\varepsilon_3'' - \varepsilon_5'')^2 + 4\tilde{V}}}, \\
 \cos 2|\gamma| &= \frac{2\tilde{V}}{\sqrt{(\varepsilon_3'' - \varepsilon_5'')^2 + 4\tilde{V}}}.
 \end{aligned} \tag{18}$$

Formulas for $|\Omega|$ can be obtained from (18) if we apply the following notations:

$$\begin{aligned}
 \varepsilon_3'' &\rightarrow 3D - \bar{h}_1, \quad \varepsilon_5'' \rightarrow 3D + \bar{h}_1, \\
 \tilde{V} &\rightarrow 3D, \quad |\gamma| \rightarrow |\Omega|, \quad \delta \rightarrow \kappa.
 \end{aligned} \tag{19}$$

Applying the scheme of diagonalization, we can represent the spin operators S^z and S^+ for HS iron ions as

$$S^z = \sum_{\lambda} \gamma_{\parallel}(\lambda) X^{\lambda} + \sum_p \Gamma_{\parallel}(p) X^{pp}, \tag{20}$$

$$S^+ = \sum_{\lambda} \gamma_{\perp}(\lambda) X^{\lambda} + \sum_p \Gamma_{\perp}(p) X^{pp},$$

where $\gamma_{\parallel}(\alpha)$, $\Gamma_{\parallel}(\alpha)$ and $\gamma_{\perp}(\alpha)$, $\Gamma_{\perp}(\alpha)$ are, respectively, the longitudinal and transverse parameters of representation of the operators S^z and S^+ in terms of the Hubbard operators. The relationship between these operators and the operators α , β , γ , and Ω is demonstrated in Appendix A. The summation over λ implies the summation over the root vectors $\lambda = \lambda(p, q)$ [32], which describe transitions from the initial state $|\psi_p\rangle$ to the final single-ion eigenstate $|\psi_q\rangle$.

LS iron ions are described by the operators $\hat{\mathcal{H}}_{0,B}$ and $\hat{\mathcal{H}}_{0,D}$, which are diagonal in the basis of eigenstates of the operators S_B^z and S_D^z , respectively. From the viewpoint of a single-ion spectrum, these ions are equivalent, and the following parameters of representation are nonzero for each of them:

$$\gamma_{\perp}(1, 2) = \Gamma_{\parallel}(1, 1) = -\Gamma_{\parallel}(2, 2) = 1/2, \tag{21}$$

where the states $|1\rangle$ and $|2\rangle$ correspond to the eigenvalues $1/2$ and $-1/2$ of the operator S^z , respectively.

The application of the atomic representation described allows us express the sum of single-site terms of Hamiltonian (2) and a correction due to exchange interaction (4) as

$$\begin{aligned}
 \hat{\mathcal{H}}_G &= \sum_{i=1}^{i=4} \sum_{f,n} E_{in} X_{fi}^{nn} \\
 &+ \sum_{i=1}^{i=4} \sum_{\langle f, f_{i+1} \rangle} \sum_{\lambda, \lambda'} (\mathbf{c}_i(\lambda), \hat{V} \cdot \mathbf{c}_{i+1}(\lambda')) \Delta X_{fi}^{\lambda} \Delta X_{f, i+1}^{\lambda'},
 \end{aligned} \tag{22}$$

where the indices i and f of the kinds of iron ions and magnetic cells to which these ions belong are recovered. Here

$$\Delta X_{fi}^{\lambda} = X_{fi}^{\lambda} - \langle X_{fi}^{\lambda} \rangle,$$

$$\begin{aligned}
 \mathbf{c}(\lambda) &= \{\gamma_{\parallel}(\lambda); \gamma_{\perp}(\lambda); \gamma_{\perp}^*(-\lambda)\}, \\
 \mathbf{c}_5(\lambda) &= \mathbf{c}_1(\lambda),
 \end{aligned}$$

and the matrix \hat{V} is given by (5).

4. GREEN'S FUNCTIONS. DERIVATION OF THE DISPERSION EQUATION

To investigate the spectral properties of the magnet (22), we apply the diagram technique for Hubbard operators [32, 37, 38]. Let us introduce the Matsubara Green's functions

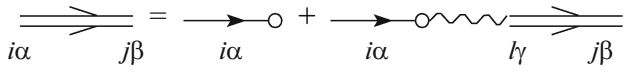


Fig. 3. Graphical representation of the system of equations for the Green's functions of a four-sublattice SCM-catenina in the loopless approximation in the (q, ω_n) -representation.

$$D_{i\alpha; j\beta}(f\tau, g\tau') = -\langle T_\tau \tilde{X}_{fi}^\alpha(\tau) \tilde{X}_{gj}^{-\beta}(\tau') \rangle$$

$$= -\frac{T}{N} \sum_{q, \omega_n} e^{i(f-g)q - i(\tau-\tau')\omega_n} D_{i\alpha; j\beta}(q; i\omega_n), \quad (23)$$

$$\tilde{X}_{fi}^\alpha(\tau) = e^{\tau H} X_{fi}^\alpha e^{-\tau H},$$

where α and β are root vectors. In the loopless approximation, the Fourier transform $D_{i\alpha; j\beta}(q, i\omega_n)$ of function (23) can be represented as [32]

$$D_{i\alpha; j\beta}(q, i\omega_n) = G_{i\alpha; j\beta}(q, i\omega_n) b_{j\beta}, \quad (24)$$

where $b_{j\alpha} = N_{jp} - N_{jq}$, and N_{jp} are the occupation numbers of the eigenstates $|\psi_{jp}\rangle$ for the ions belonging to the j th sublattice.

In the graphical form, the system of equations for the function $D_{i\alpha; j\beta}(q, i\omega_n)$ is demonstrated in Fig. 3.

Assigning analytic expressions to graphical elements, we obtain

$$G_{i\alpha; j\beta}(q; i\omega_n) = \delta_{ij} \delta_{\alpha\beta} D_{i\alpha}(i\omega_n) + D_{i\alpha}(i\omega_n) b_{i\alpha}$$

$$\times \sum_{l\gamma} V_{i(-\alpha); l\gamma}(q) G_{l\gamma; j\beta}(q; i\omega_n), \quad (25)$$

where $D_{i\alpha(n, m)}(i\omega_n) = [i\omega_n + (E_{in} - E_{im})]^{-1}$ and $V_{i\alpha; l\gamma}(q) = (\mathbf{c}_i(\alpha), \hat{V}(q) \cdot \mathbf{c}_{l\gamma}(\beta))$. Here $\hat{V}(q)$ is the Fourier transform of the matrix (5) in which the interaction between nearest neighbors was considered. Let us make use of the split form of the matrix elements $V_{i\alpha; l\gamma}(q)$ with respect to the indices of the root vectors [33, 41, 42]. Multiply Eq. (25) by $\mathbf{c}_{i\alpha}$ and sum the expression obtained over the indices i and α . Then, introducing four types of three-dimensional vectors

$$\mathbf{A}_j(\beta, i\omega_n) = \sum_{\alpha} \mathbf{c}_A(\alpha) G_{A\alpha; j\beta}(q; i\omega_n),$$

$$\mathbf{B}_j(\beta, i\omega_n) = \sum_{\alpha} \mathbf{c}_B(\alpha) G_{B\alpha; j\beta}(q; i\omega_n),$$

$$\mathbf{C}_j(\beta, i\omega_n) = \sum_{\alpha} \mathbf{c}_C(\alpha) G_{C\alpha; j\beta}(q; i\omega_n),$$

$$\mathbf{D}_j(\beta, i\omega_n) = \sum_{\alpha} \mathbf{c}_D(\alpha) G_{D\alpha; j\beta}(q; i\omega_n), \quad (26)$$

we can express the sought Greens functions as follows:

$$G_{A\alpha; j\beta}(q; i\omega_n) = \delta_{Aj} \delta_{\alpha\beta} G_{A\alpha}(i\omega_n)$$

$$+ D_{A\alpha}(i\omega_n) b_{A\alpha}(\mathbf{c}_A(-\alpha), \hat{V}(\mathbf{D}_j e^{-4iq} + \mathbf{B}_j)),$$

$$G_{B\alpha; j\beta}(q; i\omega_n) = \delta_{Bj} \delta_{\alpha\beta} G_{B\alpha}(i\omega_n)$$

$$+ D_{B\alpha}(i\omega_n) b_{B\alpha}(\mathbf{c}_B(-\alpha), \hat{V}(\mathbf{A}_j + \mathbf{C}_j)), \quad (27)$$

$$G_{C\alpha; j\beta}(q; i\omega_n) = \delta_{Cj} \delta_{\alpha\beta} G_{C\alpha}(i\omega_n)$$

$$+ D_{C\alpha}(i\omega_n) b_{C\alpha}(\mathbf{c}_C(-\alpha), \hat{V}(\mathbf{B}_j + \mathbf{D}_j)),$$

$$G_{D\alpha; j\beta}(q; i\omega_n) = \delta_{Dj} \delta_{\alpha\beta} G_{D\alpha}(i\omega_n)$$

$$+ D_{D\alpha}(i\omega_n) b_{D\alpha}(\mathbf{c}_D(-\alpha), \hat{V}(\mathbf{A}_j e^{4iq} + \mathbf{C}_j)).$$

Here the components of the vectors \mathbf{A}_j , \mathbf{B}_j , \mathbf{C}_j , and \mathbf{D}_j are determined from the system of 12 equations

$$\mathbf{A}_j = \delta_{Aj} G_{A\beta}(i\omega_n) \mathbf{c}_A(\beta) + \hat{L}_A \hat{V}(\mathbf{D}_j e^{-4iq} + \mathbf{B}_j),$$

$$\mathbf{B}_j = \delta_{Bj} G_{B\beta}(i\omega_n) \mathbf{c}_B(\beta) + \hat{L}_B \hat{V}(\mathbf{A}_j + \mathbf{C}_j), \quad (28)$$

$$\mathbf{C}_j = \delta_{Cj} G_{C\beta}(i\omega_n) \mathbf{c}_C(\beta) + \hat{L}_C \hat{V}(\mathbf{B}_j + \mathbf{D}_j),$$

$$\mathbf{D}_j = \delta_{Dj} G_{D\beta}(i\omega_n) \mathbf{c}_D(\beta) + \hat{L}_D \hat{V}(\mathbf{A}_j e^{4iq} + \mathbf{C}_j),$$

where the three-dimensional matrices \hat{L}_j ($j = A, B, C, D$) have the following components:

$$(\hat{L}_j)_{nm} = \sum_{\alpha} c_j^n(\alpha) c_j^m(-\alpha) b_{j\alpha} D_{j\alpha}(i\omega_n). \quad (29)$$

Using the representation parameters calculated in the previous section, we find that these matrices are expressed as follows:

$$L_A = \begin{pmatrix} u(i\omega) & 0 & 0 \\ 0 & w(i\omega_n) & z_A(i\omega_n) \\ 0 & z_A(-i\omega_n) & w(i\omega_n) \end{pmatrix}, \quad (30)$$

$$L_B = \begin{pmatrix} 0 & 0 & 0 \\ 0 & 0 & z_B(i\omega_n) \\ 0 & z_B(-i\omega_n) & 0 \end{pmatrix},$$

the matrix $\hat{L}_D = \hat{L}_B$, and the matrix \hat{L}_C can be obtained from the matrix \hat{L}_A by the substitution $w(i\omega_n) \rightarrow -w(i\omega_n)$. The functions appearing in these matrices have the form

$$u(i\omega_n) = \sum_{\alpha} |\gamma_{\parallel A}(\alpha)|^2 D_{A;\alpha}(i\omega_n) b_A(\alpha),$$

$$z_{A,B}(i\omega_n) = \sum_{\alpha} |\gamma_{\perp A,B}(\alpha)|^2 D_{A,B;\alpha}(i\omega_n) b_{A,B}(\alpha), \quad (31)$$

$$w(i\omega_n) = \sum_{\alpha} \gamma_{\perp A}(\alpha) \gamma_{\perp A}(-\alpha) D_{A;\alpha}(i\omega_n) b_A(\alpha).$$

Next, we use the fact that the representation parameters of iron ions in each sublattice satisfy the relation $\gamma_{\parallel}(\alpha) \gamma_{j\perp}(\pm\alpha) = 0$. Therefore, the collective excitations defined by the transverse and longitudinal parts of the exchange interaction (transverse and longitudinal vibrations) do not interact with each other.

Taking this fact into consideration, we pass from the vectors $\mathbf{A}_j(\beta, \omega_n)$, $\mathbf{B}_j(\beta, \omega_n)$, $\mathbf{C}_j(\beta, \omega_n)$, and $\mathbf{D}_j(\beta, \omega_n)$, which characterize the longitudinal and transverse vibrations of individual sublattices A , B , C , and D , to the variables that describe separately the longitudinal and transverse vibrations of the collective subsystem. These variables are given by the four-dimensional vectors

$$\begin{aligned} \mathbf{Z}_j &= \{\mathbf{A}_j^1; \mathbf{B}_j^1; \mathbf{C}_j^1; \mathbf{D}_j^1\}, \\ \mathbf{P}_j^{+(-)} &= \{\mathbf{A}_j^{2(3)}; \mathbf{B}_j^{2(3)}; \mathbf{C}_j^{2(3)}; \mathbf{D}_j^{2(3)}\}. \end{aligned} \quad (32)$$

The vector $\mathbf{Z}_j(\beta, i\omega_n)$ describes only longitudinal vibrations of SCM-catenas. Direct calculations show that $\mathbf{Z}_j(\beta, i\omega_n) = 0$ for the system considered. This means that longitudinal magnon excitations do not contribute to the spectral and thermodynamic properties of the system and that one should consider only transverse magnetic excitations described by the vectors $\mathbf{P}_j^\pm(\beta, i\omega_n)$. The latter are determined from the following system of equations:

$$\begin{aligned} \begin{pmatrix} \mathbf{P}_j^+ \\ \mathbf{P}_j^- \end{pmatrix} &= \begin{pmatrix} \hat{\Phi}(q, i\omega_n) & \hat{W}(q, i\omega_n) \\ \hat{W}(q, i\omega_n) & \hat{\Phi}(q, -i\omega_n) \end{pmatrix} \\ &\times \begin{pmatrix} \mathbf{P}_j^+ \\ \mathbf{P}_j^- \end{pmatrix} = \begin{pmatrix} \mathbf{y}_{j\perp}(\beta, i\omega_n) \\ \mathbf{y}_{j\perp}(-\beta, -i\omega_n) \end{pmatrix}, \end{aligned} \quad (33)$$

where the i th components of the four-dimensional vectors $\mathbf{y}_{j\perp}(\beta, \omega_n)$ are given by

$$y_{j\perp}^i(\beta, \omega_n) = \delta_{ij} \gamma_{\perp j}(\beta) D_{j\beta}(\omega_n),$$

while the four-row matrices \hat{U} and \hat{W} have the form

$$\begin{aligned} \hat{\Phi} &= \frac{J}{2} \begin{pmatrix} -1 & z_A & 0 & z_A e^{-4iq} \\ z_B & -1 & z_B & 0 \\ 0 & z_A & -1 & z_A \\ z_B e^{4iq} & 0 & z_B & -1 \end{pmatrix}, \\ \hat{W} &= \frac{J}{2} \begin{pmatrix} 0 & w & 0 & w e^{-4iq} \\ 0 & 0 & 0 & 0 \\ 0 & -w & 0 & -w \\ 0 & 0 & 0 & 0 \end{pmatrix}. \end{aligned} \quad (34)$$

The solution of Eqs. (33) with the use of (27) and (32) allows us to calculate the collective Green's functions (23). In the present paper, we display the calculated Green's functions for two of the four sublattices (the sublattices A and B), one of which describes HS, and the other, LS ions of iron:

$$\begin{aligned} D_{A\alpha; A\beta}(q, i\omega_n) &= D_{A\beta}(i\omega_n) b_A(\beta) \delta_{\alpha\beta} \\ &+ J_q D_{A\alpha}(i\omega_n) D_{A\beta}(i\omega_n) b_A(\alpha) b_A(\beta) \\ &\times \left(\left[\frac{\gamma_{\perp A}(-\alpha)}{\Delta_{\perp}(q, i\omega_n)} (\gamma_{\perp A}(-\beta) \tilde{M}_{12}(q, \omega_n) \right. \right. \\ &\left. \left. + \gamma_{\perp A}(\beta) \tilde{M}_{52}(q, \omega_n) \right] + \left[\begin{array}{l} \alpha \rightarrow -\alpha; \beta \rightarrow -\beta \\ i\omega_n \rightarrow -i\omega_n \end{array} \right] \right) \end{aligned} \quad (35)$$

for sublattice A , and

$$\begin{aligned} D_{B\alpha; B\beta}(q, i\omega_n) &= D_{B\beta}(i\omega_n) b_B(\beta) \delta_{\alpha\beta} \\ &+ J_q D_{B\alpha}(i\omega_n) D_{B\beta}(i\omega_n) b_B(\alpha) b_B(\beta) \\ &\times \left(\left[\frac{\gamma_{\perp B}(-\alpha)}{\Delta_{\perp}(q, i\omega_n)} (\gamma_{\perp B}(-\beta) \tilde{M}_{21}(q, i\omega_n) \right. \right. \\ &\left. \left. + \gamma_{\perp B}(\beta) \tilde{M}_{61}(q, i\omega_n) \right] + \left[\begin{array}{l} \alpha \rightarrow -\alpha; \beta \rightarrow -\beta \\ i\omega_n \rightarrow -i\omega_n \end{array} \right] \right) \end{aligned} \quad (36)$$

for sublattice B . We do not present the Green's functions for sublattices C and D , because, in what follows, we will calculate single-ion occupation numbers N_{jp} of the system, the determination of which requires the Green's functions $D_{j\alpha; j\alpha}$ that are diagonal with respect to the indices of root vectors of the sublattices. These functions satisfy the relations $D_{A\alpha; A\alpha} = D_{C\alpha; C\alpha}$ and $D_{B\alpha; B\alpha} = D_{D\alpha; D\alpha}$.

The functions $\tilde{M}_{12}(q, i\omega_n)$, $\tilde{M}_{52}(q, i\omega_n)$, $\tilde{M}_{21}(q, i\omega_n)$, and $\tilde{M}_{61}(q, i\omega_n)$ in (35) and (36) are determined in terms of the minors $M_{ij}(q, i\omega_n)$, which are obtained by deleting the i th row and the j th column of the matrix appearing in the system of equations (33):

$$\begin{aligned} \tilde{M}_{12} &= M_{12} + M_{14} e^{-4iq} = 2 \operatorname{Re} M_{12}, \\ \tilde{M}_{52} &= M_{52} + M_{54} e^{-4iq} = 2 \operatorname{Re} M_{52}, \\ \tilde{M}_{21} &= M_{21} + M_{23} = 2 \operatorname{Re} M_{21}, \\ \tilde{M}_{61} &= M_{61} + M_{63} = 2 \operatorname{Im} M_{61}, \end{aligned} \quad (37)$$

where Re and Im denote the real and imaginary parts of appropriate expressions. The explicit form of functions (37) is presented in Appendix B. One can verify that the Green's functions thus calculated possess necessary symmetry properties: $D_{j\alpha; j\beta}(q, i\omega_n) = D_{j\beta; j\alpha}^*(q, i\omega_n)$, and $D_{j\alpha; j\beta}(q, i\omega_n) = D_{j(-\beta); j(-\alpha)}(q, -i\omega_n)$.

The denominator $\Delta(q, i\omega_n)$ of Green's functions (35) and (36) can be expressed as

$$\begin{aligned} \Delta_{\perp}(q, i\omega_n) &= \tilde{\Delta}_{\perp}(q, i\omega_n) \tilde{\Delta}_{\perp}\left(q + \frac{\pi}{2}; i\omega_n\right) \\ &+ \frac{J}{2} z_B(i\omega_n) z_B(-i\omega_n) w^2(i\omega_n) (1 + \cos 4q), \end{aligned} \quad (38)$$

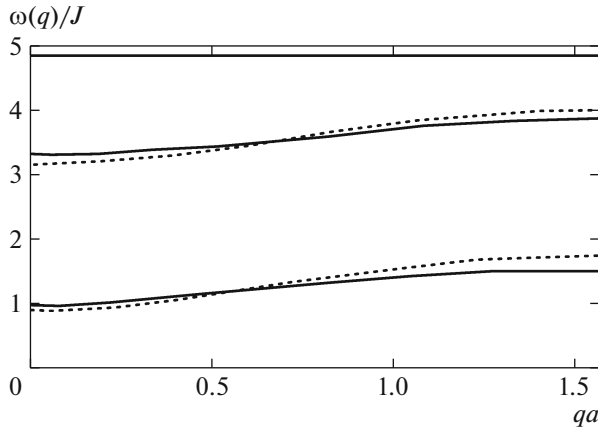


Fig. 4. Low-temperature spectrum of elementary excitations of the four-sublattice ferrimagnet SCM-catena for $D/J = 3/8$ (solid lines). The dotted lines illustrate the excitation spectrum obtained by formula (42) for a ferrimagnet in which anisotropy with alternating easy magnetization planes is replaced by the effective easy-axis anisotropy with $D_{\text{eff}}/J = -1/8$.

where

$$\begin{aligned} \tilde{\Delta}_{\perp}(q, i\omega_n) = & \left[1 - \left(\frac{J_q}{2} \right)^2 z_A(i\omega_n) z_B(i\omega_n) \right] \\ & \times \left[1 - \left(\frac{J_q}{2} \right)^2 z_A(-i\omega_n) z_B(-i\omega_n) \right] \\ & + \left(\frac{J_q}{2} \right)^4 z_B(i\omega_n) z_B(-i\omega_n) w^2(i\omega_n). \end{aligned} \quad (39)$$

The equation $\Delta_{\perp}(q, i\omega_n \rightarrow \omega + \delta) = 0$ defines the spectrum of elementary excitations of SCM-catena in the approximation considered.

5. LOW-TEMPERATURE SPECTRAL PROPERTIES. QUANTUM RENORMALIZATIONS OF SINGLE-ION OCCUPATION NUMBERS

As mentioned, the experimental investigations of SCM-catena show that, at low temperatures, this compound exhibits properties characteristic of magnets with easy-axis anisotropy, or even of magnets with dominant Ising-type exchange. This assertion can be proved by considering the specific features of the spectrum of magnetic excitations.

In the low-temperature limit ($T \ll J$), there are six transitions that determine collective branches: two transitions from each HS iron ions $|\psi_{A,C}^1\rangle \leftrightarrow |\psi_{A,C}^2\rangle$ and $|\psi_{A,C}^1\rangle \leftrightarrow |\psi_{A,C}^4\rangle$, as well as one transition for each LS ion $|\psi_{B,D}^1\rangle \leftrightarrow |\psi_{B,D}^2\rangle$. The quasimomentum dependence of these branches is determined within the first Brillouin zone: $-\pi/4a \leq q \leq \pi/4a$, where $a \approx 10 \text{ \AA}$. To

compare this spectrum with the excitation spectrum obtained in the model of easy-axis magnet with two sublattices, it is convenient to consider quasiparticle branches defined in the extended interval of quasimomenta $-\pi/2a \leq q \leq \pi/2a$. Taking account of the relation $\Delta_{\perp}(q, \omega) = \Delta_{\perp}(q + \pi/2, \omega)$, which follows from (38), we rewrite the denominator of the Green's function:

$$\begin{aligned} \Delta_{\perp}(q, \omega) & \sim \prod_{j=1}^6 (\omega^2 - \omega_j^2(q)) \\ & = \prod_{j=1}^3 (\omega^2 - \omega_j^2(q)) \left(\omega^2 - \omega_j^2\left(q + \frac{\pi}{2}\right) \right), \end{aligned} \quad (40)$$

where $-\pi/4 \leq q \leq \pi/4$. We can see that the determination of six branches of the spectrum of SCM-catena that are defined within the first Brillouin zone of a four-sublattice magnet is equivalent to determining three branches, defined in the first Brillouin zone, for a two-sublattice magnet: $-\pi/2 < q < \pi/2$.

The dispersion relations of three quasiparticle branches constructed in the interval $0 \leq q \leq \pi/2$ for $T \ll J$ and for the experimentally established relation between the exchange and anisotropy parameters for the given compound ($D/J = 3/8$) are demonstrated by solid lines in Fig. 4. The dotted lines in this figure illustrate the quasimomentum dependence of the branches of the spectrum for the effective model of a two-sublattice ferrimagnetic Heisenberg chain with easy-axis single-ion anisotropy. It is assumed that such a model is described by the Hamiltonian

$$\begin{aligned} \hat{\mathcal{H}}_{\text{eff}} & = \sum_{f_1 \in A} \hat{\mathcal{H}}_{0,A}(f_1) + \sum_{f_2 \in B} \hat{\mathcal{H}}_{0,B}(f_2) + \hat{\mathcal{H}}_{\text{int}}, \\ \hat{\mathcal{H}}_{0,A}(f_1) & = 2D_{\text{eff}}(S_{f_1}^z)^2 + \bar{h}_1 S_{f_1}^z, \end{aligned} \quad (41)$$

where $\hat{\mathcal{H}}_{0,B}(f_2)$ and $\hat{\mathcal{H}}_{\text{int}}$ are defined by expressions (3) and (4), respectively. In this case, one should change the summation over four sublattices in expression (4) for $\hat{\mathcal{H}}_{\text{int}}$ to the summation over two sublattices. The analytic expressions for the quasimomentum dependence of the branches of the spectrum of such a model for $T \ll J$ are given by

$$\begin{aligned} \tilde{\omega}_{1,2}(q) & = \pm b + \sqrt{b^2 - a(q)}, \\ a(q) & = (2D_{\text{eff}}(2S_A - 1) + 2JS_B) \\ & \times (2D_{\text{eff}}(2S_B - 1) + 2JS_A) + J_q^2 S_A S_B, \\ b & = 2D_{\text{eff}}(S_A + S_B - 1) - J(S_A - S_B). \end{aligned} \quad (42)$$

When constructing the quasimomentum dependence in Fig. 4, we took the following values of the parameters: $S_A = 2$, $S_B = 1/2$, and $D_{\text{eff}} = -J/8$. The comparison of the functions presented in Fig. 4 shows that, at low temperatures, the excitation spectrum of SCM-catena indeed corresponds to the spectrum of one-dimensional ferrimagnet with the effective easy-

magnetization axis directed along the axis of the chain. Moreover, in both models, the excitation spectrum is characterized by a gap of $\Delta \sim J$ and a small, compared to Δ , dispersion of the main excitation branches. This means that the energy spectrum of excitations of the one-dimensional four-sublattice ferrimagnet SCM-catenana is well reproduced by a single-particle spectrum of excitations of a ferrimagnetic Ising chain, for which also $\Delta \sim J$ and the dispersion of the branches is missing completely. This important conclusion allows us to pass to the study of the thermodynamic properties of SCM-catenana in the entire temperature interval on the basis of the exact calculation of the statistical sum for the effective generalized one-dimensional Ising model.

However, a more correct transition to the effective model requires that one should take into account strongly developed spin fluctuations in the system, which are not described within Ising-type models. In the original Hamiltonian of SCM-catenana (1), the main contribution to the development of these fluctuations is made by the terms describing the single-ion anisotropy of the system. It is known that, due to the presence of this kind of terms in the Hamiltonian of a spin subsystem, the full description of its magnetic state requires the introduction of single-site means of the type $\langle S_{\alpha_1} S_{\alpha_2} \cdot S_{\alpha_n} \rangle$ ($\alpha_i = x, y, z$ and $n \leq 2S$) that correspond to dipole ($n = 1$), quadrupole ($n = 2$), etc. order parameters. The implementation of states with nonzero means of this type leads to quantum effects that may significantly tell on the spectral properties and the phase diagram of the system [3, 35, 39], as well as on the specific features of its dynamics [40]. Among such effects, one should distinguish the so-called quantum reduction of spin. This effect manifests itself in that the mean value of the projection of the spin moment to the axis of quantization, $\langle S^z \rangle$, turns out to be less in absolute value than the nominal value of spin at the site, $|\langle S^z \rangle| < S$, even at zero temperature [35]. In the present study, we restrict ourselves to the analysis of the effect of quantum fluctuations in SCM-catenana on $\langle S^z \rangle$.

To take into account the effect of spin fluctuations, one should go beyond the framework of mean-field approximation and take into account the contribution of spin-wave renormalizations to single-ion occupation numbers of iron ions. To this end, we consider the definition of the occupation numbers:

$$\begin{aligned} N_{jp} &= -\langle T_\tau \tilde{X}_{jj}^{\alpha(r,p)}(\tau) X_{jj}^{-\alpha(r,p)}(\tau + \delta) \rangle \\ &= -\frac{T}{N} \sum_{q, \omega_n} e^{i\delta\omega_n} D_{j\alpha; j\alpha}(q, \omega_n), \end{aligned} \quad (43)$$

where $\delta \rightarrow 0^+$, $j = A, B$, and the root vectors $\alpha = \alpha_j(r, p)$ describe the above-considered transitions between the magnetic states of iron ions for which the original sum of occupation numbers is different from zero. $D_{j\alpha; j\alpha}$ are

the Green's functions obtained in (35) and (36). It is important that these functions can be represented as

$$D_{j\alpha; j\alpha}(q, i\omega_n) = \frac{F_j(\alpha, q, i\omega_n)}{6 \prod_{k=1} ((i\omega_n)^2 - \omega_k^2(q))}, \quad (44)$$

where $F_j(\alpha, q, i\omega_n)$ is a polynomial function of the variable $i\omega_n$. This allows us to pass from the summation over Matsubara frequencies in (43), which take values of $\omega_n = 2\pi nT$ ($n = 0, \pm 1, \pm 2, \dots$), to the integration along a special contour with respect to the complex variable $\omega = \omega' + i\omega''$ and to rewrite the expression for the occupation numbers as

$$\begin{aligned} N_{jp} &= \frac{1}{2N} \sum_{q,k} \frac{(F_j(\alpha, q, \omega_k) + F_j(\alpha, q, -\omega_k)) f_B\left(\frac{\omega_k}{T}\right)}{\omega_k \prod_{p \neq k} (\omega_p^2 - \omega_k^2)} \\ &\quad + \frac{1}{2N} \sum_{q,k} \frac{F_j(\alpha, q, -\omega_k)}{\omega_k \prod_{p \neq k} (\omega_p^2 - \omega_k^2)}, \end{aligned} \quad (45)$$

where $q \in [-\pi/4a, \pi/4a]$, $\omega_k(q)$ is the k th branch of the excitation spectrum of SCM-catenana, and $f_B(\omega/T) = [\exp(\omega/T) - 1]^{-1}$ is the Bose–Einstein distribution function. The last term in expression (45) is independent of temperature and is responsible for the quantum renormalizations of occupation numbers. The latter renormalizations also lead to the variation of the mean value of magnetization in the system. The analysis has shown that a significant modification of this parameter is implemented only for iron ions in HS states; therefore, below we will consider precisely these iron ions. If we take into account that, at zero temperature, only the second and fourth of the eigenstates (13) of HS ions of iron experience quantum renormalizations, then the expression for the mean value of the spin magnetic moment of these ions in the spin-wave approximation has the form

$$\begin{aligned} \langle S_{A,C}^z \rangle_{s-w} &= N_1 \langle \Psi_1 | S_{A,C}^z | \Psi_1 \rangle + N_2 \langle \Psi_2 | S_{A,C}^z | \Psi_2 \rangle \\ &\quad + N_4 \langle \Psi_4 | S_{A,C}^z | \Psi_4 \rangle. \end{aligned} \quad (46)$$

Note that if the calculations of the quantum reduction of spin were performed in the mean-field approximation, then the expression for $\langle S_{A,C}^z \rangle$ would have the form

$$\langle S_{A,C}^z \rangle_{mf} = \langle \Psi_1 | S_{A,C}^z | \Psi_1 \rangle. \quad (47)$$

The dependence of $\langle S_{A,C}^z \rangle$ for HS ions of iron on the value of anisotropy calculated on the basis of formulas (46) and (47) is illustrated in Fig. 5 by solid and dotted curves, respectively. The solid vertical lines indicate the experimental values of anisotropy for SCM-catenana. One can see that, for $D/J = 3/8$, the

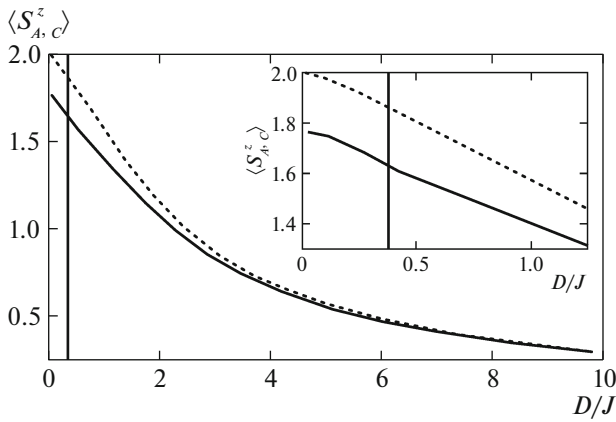


Fig. 5. Mean value of the magnetic moment of HS ions as a function of anisotropy in the low-temperature limit $T \ll J$. The dotted curves illustrate the dependence of $\langle S_{HS}^z \rangle$ on D calculated in the mean-field approximation. The solid curves represent the dependence obtained when spin-wave renormalizations of single-ion occupation numbers are taken into consideration. The vertical line points to the value of the anisotropy-to-exchange ratio $D/J = 3/8$ in SCM-catena borrowed from experimental data.

mean projection of the spin moment onto the axis of quantization takes a value of $\langle S_{A,C}^z \rangle \approx 1.63$, more than $2/3$ of the contribution to the relative variation of the magnetization of HS ions being due to spin-wave fluctuations.

6. EFFECTIVE MODEL. PHOTOINDUCED CHANGE OF ONE-DIMENSIONAL MAGNET AND A STATISTICAL ENSEMBLE OF ISING CHAINS

The specific features of the spectrum of magnetic excitations and magnetization curves considered above allow one to suggest that, at temperatures $T \sim J$, the magnetic properties of the compound can be described within the model of a spin chain with alternating pseudospin moments $\tilde{S} = 3/2$ and $\sigma = 1/2$ between which an Ising-type exchange interaction is implemented. This fact can be confirmed by the results of exact calculation for a finite number of sites, which are represented in Fig. 6. The solid curves represent the temperature dependence of the induced magnetic moment on the magnetic field (for two orientations of this field) for an anisotropic Heisenberg chain of six sites described by Hamiltonian (1) for SCM-catena. The dotted curves demonstrate the same dependence calculated on the basis of a generalized Ising model described by the Hamiltonian

$$\hat{\mathcal{H}}_I = J \sum_{f=1}^6 (\tilde{S}_f^z \tilde{S}_{f+1}^z - \mathbf{h} \cdot \tilde{\mathbf{S}}_f), \quad (48)$$

$$\tilde{S}^z = \text{diag}(2, 1, 0, -1, -2).$$

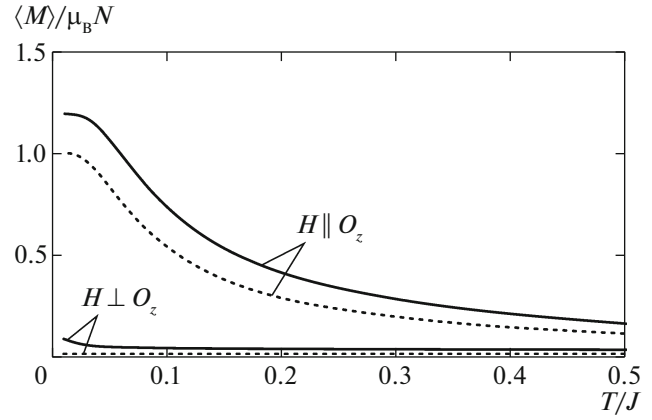


Fig. 6. Temperature dependence of the site magnetization $M(T)$ for chains of six sites for various orientations of the external magnetic field. The solid curves correspond to calculations within the Heisenberg anisotropic model (1) for $D/J = 3/8$, and the dotted curves correspond to similar calculations within the Ising model (48).

The comparison of the curves shows that, in the range of parameters of interest, the application of the Ising model allows one to well reproduce the properties of SCM-catena both for a magnetic field applied along the chain and for a field applied perpendicular to the chain.

To analyze the effect of optical irradiation on the magnetic properties of SCM-catena, we take into account that, in MMCT processes (Fig. 2), HS iron ions go over to the state Fe^{III} ($S = 5/2$), and LS ions, to the state Fe^{II} ($S = 0$). We will model the emergence of such iron ions by introducing magnetic impurities into the chain, whose concentration depends on the radiation intensity. In addition, we will take into account the presence of impurities and defects of natural origin. Here, it is important that the description of the magnetic properties of the compound will take into account the characteristic times of the dynamics of the impurities, both photoinduced ones and impurities that arise at technological level.

It is customary to assume that the characteristic times of the dynamics of impurities and defects of natural origin are much greater than the characteristic times of the dynamics of the magnetic subsystem. This means that such defects implement a “quenched” type of disorder [6]. Moreover, in most single-chain magnets, such inclusions have a relatively low concentration ($c \sim 10^{-3} - 10^{-2}$ per unit length of the chain); therefore, these inclusions are distributed uniformly over the chain and are not correlated. According to the aforesaid, we can assume that the detection probability P_N of a chain with the number of sites N in a sample obeys the Poisson statistics: $P_N = \bar{N}^N e^{-\bar{N}} / N!$. Here \bar{N} defines the average number of particles in a segment of the chain bounded by nonmagnetic impurities.

Further, it is essential that, during experimental investigations of the effect of light on single-chain magnets, the irradiation lasted for several hours [8, 25, 26]. During this period, photoinduced HS Fe^{III} and LS Fe^{II} states of iron ions arise and recombine repeatedly. Therefore, on average, each iron ion takes part in MMCT processes and, while remaining in its place, changes its state due to the arrival and departure of electrons. This feature can be reproduced by introducing a special statistical ensemble whose representatives are spin chains. The sites of the chain can be occupied by iron ions in any of the four spin states introduced above. This approach allows one to take into account the appearance of photoinduced impurities in the chains and corresponds to the description of magnets with “annealed” type of disorder [49]. The introduction of a statistical ensemble implies establishing a material contact with a thermostat that admits exchange of iron ions and thereby simulates a variation in the relative concentration of ion pairs in different spin states. Finally, we take into account that, due to the quantum fluctuations, the projection of the spin moment S^z of iron ions in the HS Fe^{III} state with total spin of $S = 5/2$ also decreases to the effective value $\tilde{S}_2 \approx 2$.

Taking into account the aforesaid, we obtain a model that is given by a Hamiltonian of the form

$$\hat{\mathcal{H}} = \sum_{f=1}^N \{ \mathcal{H}(f, f+1) + \hat{\mathcal{H}}(f+1, f) \} + \sum_{f=1}^N \{ \mu_B H \hat{O}_f + \lambda_1 h_f + \lambda_2 Y_f \} \quad (49)$$

in the atomic representation, where two-site operators represent a sum of two terms,

$$\hat{\mathcal{H}}(f, f+1) = \hat{\mathcal{H}}_J(f, f+1) + \hat{\mathcal{H}}_V(f, f+1). \quad (50)$$

The operators $\hat{\mathcal{H}}_J(f, f+1)$ describe an Ising-type exchange interaction between nearest neighbor magnetically active iron ions:

$$\hat{\mathcal{H}}_J(f, g) = J_1 \sum_{mM} m M X_f^{mm} Y_g^{MM} + J_2 \sum_{mL} m L X_f^{mm} Z_g^{LL}. \quad (51)$$

Here the operators Y_f^{mm} (Y_f^{MM}) are Hubbard operators [37] of projection onto the vectors of a Hilbert space that correspond to the states of iron ions with spin (pseudospin) $S = 1/2$ ($\tilde{S} = 3/2$) and the projection m (M) of spin (pseudospin) onto the axis of quantization. The projection operator Z_f^{LL} corresponds to the state of an iron ion at site f with $\tilde{S}_2 = 2$ and the projection L of pseudospin onto the axis of quantization.

The operator h_f is a Hubbard operator of projection onto the vector $|f, 0\rangle$ of a Hilbert space, that corresponds to the position of the iron ion at site f in the state with spin $S = 0$. As pointed out above, the states described by the operators Z_f^{LL} and h_f arise as a result of optical irradiation. Here, it is assumed that $M = 0.5\{3; 1; -1; -3\}$ and $L = \{2; 1; 0; -1; -2\}$ for HS ions of iron.

The bivalent operators $\hat{\mathcal{H}}_V$ are introduced to take into account the correlation in the arrangement of iron ions of different types (see Figs. 1 and 2) and allow one to reproduce a necessary sequence of spin states of iron ions that corresponds to the magnetic structure of SCM-catena. These operators describe a repulsive interaction within pairs of HS (LS) iron ions located at the nearest neighbor sites of the chain. In the atomic representation, the expression for $\hat{\mathcal{H}}_V$ is given by

$$\hat{\mathcal{H}}_V(f, g) = V(h_f h_g + X_f X_g + Y_f Y_g + Z_f Z_g + h_f X_g + Y_f Z_g), \quad (52)$$

where the operators

$$X_f = \sum_m X_f^{mm}, \quad Y_f = \sum_M Y_f^{MM}, \quad Z_f = \sum_L Z_f^{LL}$$

are projection operators onto subspaces with fixed values of spin or pseudospin without indicating its projection. The parameter V characterizes the amplitude of the repulsive interaction and is assumed to be infinitely large in final calculations.

The first term among single-site operators in (49) represents the Zeeman contribution and, in the notation adopted,

$$\hat{O}_f = g_1 \sum_m m X_f^{mm} + g_2 \sum_M M Y_f^{MM} + g_3 \sum_L L Z_f^{LL}, \quad (53)$$

where g_1 , g_2 , and g_3 are the g factors for each of the three magnetic states of iron ions.

The appearance of the last two single-site operators in (49) is associated with the fact that irradiation is accompanied by a simultaneous transition of a pair of iron ions to new states. Mathematically, this fact is reflected by the equations

$$\langle X_f \rangle = \langle Y_f \rangle, \quad \langle h_f \rangle = \langle Z_f \rangle. \quad (54)$$

To take into account these conditions, we introduce two undetermined Lagrange multipliers λ_1 and λ_2 that allow us to control the average number of iron ions in different spin states. These multipliers are usually determined at the final state of calculations from the requirement that relations (54) should be satisfied.

The statistical sum for the ensemble of chains introduced is calculated by the transfer-matrix method [19, 43–47]. Compared with other methods [48, 49] for solving the problem of the effect of annealed disorder on the magnetic properties of the

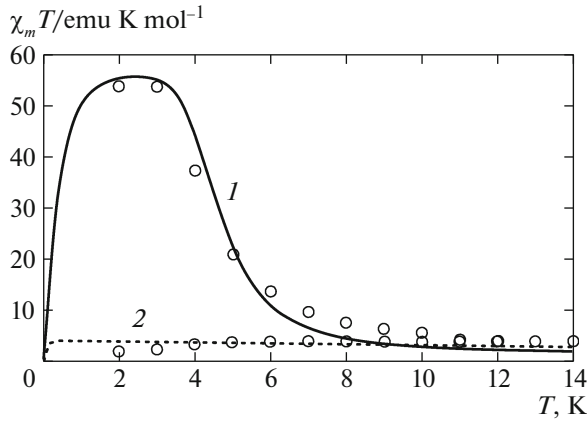


Fig. 7. Modification of the temperature dependence of the magnetic susceptibility of SCM-catena in the absence of radiation (theory (solid curve 1) and experiment (circles)) and under irradiation (theory (dotted curve 2) and experiment (circles)). The experimental data are borrowed from [27], and the calculation parameters of the model are defined by relations (58).

Ising model, the approach based on the transfer-matrix technique allows one to carry out straightforward calculations of both the means

$$\langle A_f^{(v)} \rangle_N = \frac{1}{\Xi} \sum_{\alpha=1}^{12} \langle u_\alpha | A^{(v)} | u_\alpha \rangle \lambda_\alpha^N \quad (55)$$

and the correlation functions

$$\begin{aligned} & \langle A_f^{(v_1)} A_{f+1}^{(v_2)} \dots A_{f+k-1}^{(v_k)} \rangle_N \\ &= \frac{1}{\Xi} \sum_{\alpha_1 \dots \alpha_k=1}^{12} A_{\alpha_1 \alpha_2}^{(v_1)} A_{\alpha_2 \alpha_3}^{(v_2)} \dots A_{\alpha_k \alpha_1}^{(v_k)} \lambda_{\alpha_1}^{N-k} \lambda_{\alpha_2} \dots \lambda_{\alpha_k}, \end{aligned} \quad (56)$$

constructed on the operators $A_f^{(v)}$ that are diagonal in the space of single-site states of the chain. The index v numbers the type of the single-site operator $A_f^{(v)}$. In this paper, we take linear combinations of the operators $X_f^{mm}, Y_f^{MM}, Z_f^{LL}$, and h_f as $A_f^{(v)}$. The quantities $|u_\alpha\rangle$ and λ_α are the eigenvectors and eigenvalues of the transfer matrix, respectively. Here $A_{\alpha,\beta}^{(v)}$ is the matrix of the operator $A^{(v)}$ in the chosen basis of eigenvectors: $A_{\alpha,\beta}^{(v)} = \langle u_\alpha | A^{(v)} | u_\beta \rangle$.

When analyzing the effect of radiation on the magnetic properties of SCM-catena, the concentration n_{hv} of photons that induce MMCT processes is identified with the means: $n_{hv} = \langle h_f \rangle = \langle Z_f \rangle$. The variation in the radiation intensity is modeled by the variation of n_{hv} ; it is assumed that $n_{hv} = 0$ in the absence of radiation. Accordingly, for every fixed value of radiation intensity, the averages are calculated by (55) and (56) simultaneously with the solution of system (54).

7. RESULTS OF NUMERICAL CALCULATIONS. MODIFICATION OF MAGNETIC PROPERTIES UNDER IRRADIATION

The expressions for the thermodynamic means (55) obtained by the transfer-matrix method allow one to describe the experimentally observed modification of the temperature dependence of the magnetic susceptibility of SCM-catena under optical irradiation within the effective model. Moreover, the expressions for the correlation functions (56) allow one to analyze the variations in the magnetic structure of the compound subjected to irradiation. The modification of the molar susceptibility $\chi_m(T)$ under irradiation of SCM-catena is demonstrated in Fig. 7. The temperature dependence of $\chi_m(T)$ for a given concentration n_{hv} is calculated by the formula

$$\chi_m(T) = N \mu_B \frac{\partial}{\partial H} \sum_N \frac{\bar{N}^N e^{-\bar{N}}}{N!} \langle \mathbb{O}_f \rangle_N. \quad (57)$$

It turns out that the following set of parameters of the effective model are the best from the viewpoint of agreement between the theoretical results on the modification of $\chi_m(T)$ and experimental data:

$$\begin{aligned} J_1 &= 7 \text{ K}, & J_2 &= 15 \text{ K}, \\ \bar{N} &= 78, & H &= 100 \text{ Oe}, \\ g_1 &= 3.1, & g_2 &= 2.9, & g_3 &= 2.5. \end{aligned} \quad (58)$$

These results well correlate with known experimental data on the system [27, 31]:

$$\begin{aligned} J &\approx 10 \text{ K}, & g_{1,2,3} &\approx 2, \\ \bar{N} &\sim 100, & H &\approx 100 \text{ Oe}, \end{aligned} \quad (59)$$

Let us dwell on the cause of the above modification of the function $\chi_m(T)T$ under irradiation. In the absence of radiation, the function $\chi_m(T)T$, shown by the solid curve in Fig. 7, is typical of an Ising-type ensemble of chains [43], and the appearance of a peak at $T \sim J$ points to the destruction (appearance) of short-range magnetic order in the system. As the radiation intensity increases, the amplitude of the peak decreases, which is associated with the appearance of iron ions in the zero-spin state. The induction of such ions is accompanied by breaking the exchange bonds in the chain and gives rise to paramagnetic centers in the chain. The latter centers are formed when two nearest neighbor LS iron ions occur in a nonmagnetic state, while the HS iron ion in between them is isolated from the magnetic viewpoint. As is known, the temperature dependence of the susceptibility of the ensemble of such paramagnetic centers obeys the Curie–Weiss law, for which the product $\chi_m(T)T$ is constant ($T_N = 0$). Under sufficiently strong irradiation, the contribution of this set of isolated HS iron ions to the magnetic susceptibility becomes dominant,

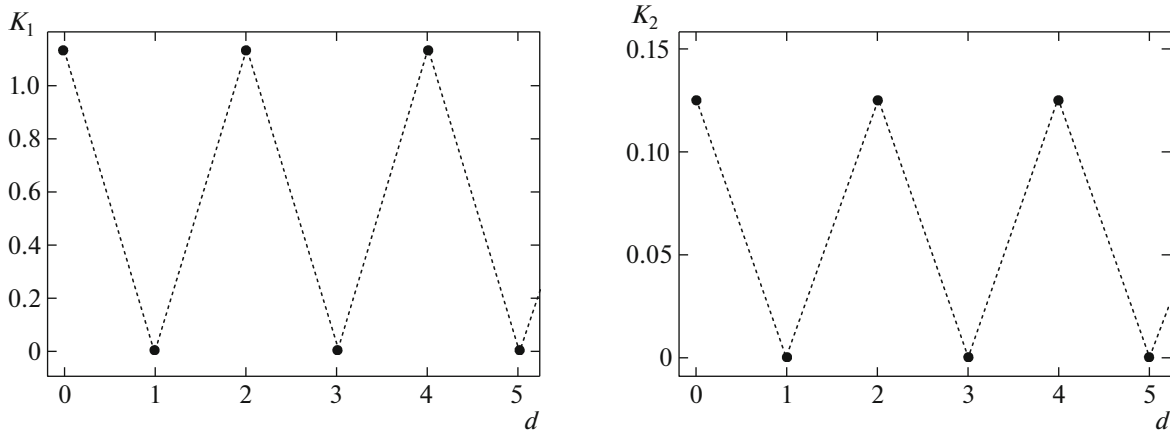


Fig. 8. Spin correlators as a function of the distance d between sites in the absence of radiation ($n_{hv} = 0$) in the low-temperature limit: (a) magnetic correlations are calculated for a pair of HS iron ions, $K_1(d) = \langle S_{HS}^z(f)S_{HS}^z(f+d) \rangle$ and (b) magnetic correlations are calculated for a pair of LS iron ions, $K_2(d) = \langle S_{LS}^z(f)S_{LS}^z(f+d) \rangle$. These functions are characteristic of a completely ordered ferrimagnetic Ising chain with alternating moments $\tilde{S} = 3/2$ and $\sigma = 1/2$.

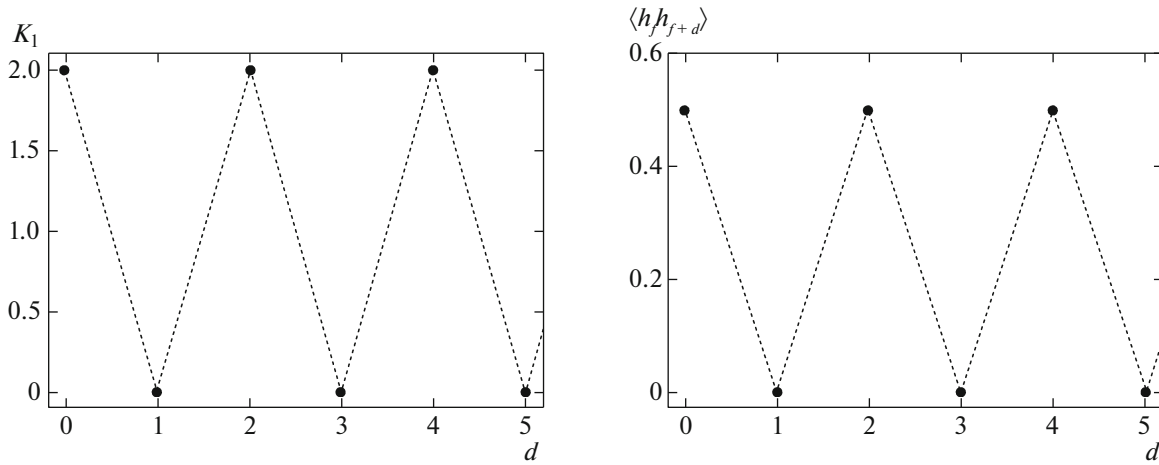


Fig. 9. Single-site correlators as a function of the distance d between sites in the case of superstrong radiation ($n_{hv} = 0.5$) in the low-temperature limit: (a) spin correlator $K_1(d) = \langle S_{HS}^z(f)S_{HS}^z(f+d) \rangle$ between a pair of HS iron ions, and (b) correlator $\langle hf_{f+d} \rangle$ characterizing iron ions in nonmagnetic states. These functions are characteristic of an ordered one-dimensional set of isolated magnetic centers with moments of $\tilde{S}_2 = 2$ between which nonmagnetic centers are located.

and the product $\chi_m(T)T$ remains the same for any temperature; this is illustrated by the dotted line in Fig. 7.

This interpretation is confirmed, in particular, by the results of calculation of the correlation functions

$$\begin{aligned} K_1(d) &= \langle S_{HS}^z(f)S_{HS}^z(f+d) \rangle, \\ K_2(d) &= \langle S_{LS}^z(f)S_{LS}^z(f+d) \rangle \end{aligned} \quad (60)$$

for various values of n_{hv} . The operators appearing in these functions have the following structure:

$$\begin{aligned} S_{HS}^z(f) &= \sum_M MY_f^{MM} + \sum_L LZ_L^{LL}, \\ S_{LS}^z(f) &= \sum_m mX_f^{mm}. \end{aligned} \quad (61)$$

Figure 8 demonstrates $K_1(d)$ and $K_2(d)$ as a function of the distance d between the sites of the chain in the absence of radiation, when $n_{hv} = 0$. The function $K_1(d)$ describes magnetic correlations between two HS

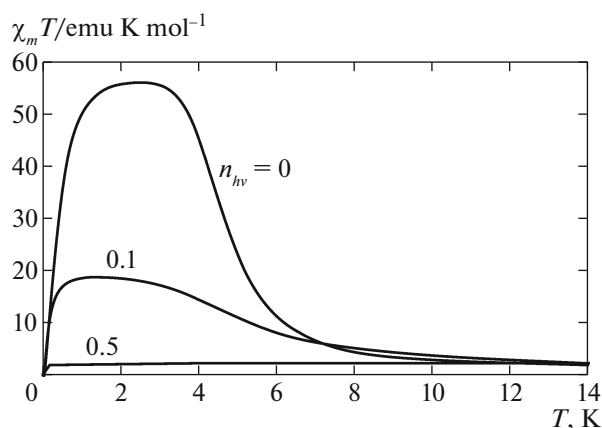


Fig. 10. Temperature dependence of the magnetic susceptibility of the system for various intensities of optical radiation. The parameters of the model are given in (58).

ions of iron located at sites with indices f and $f + d$. Similarly, the function $K_2(d)$ describes spatial magnetic correlations of LS ions of iron. One can see that $K_1(d)$ ($K_2(d)$) takes values equal to $0.5\sigma^2$ ($0.5\tilde{S}^2$) for even d and zero for odd d . The factor $1/2$ in the expressions for even d is attributed to the presence of two kinds of iron ions: HS and LS ions. This spatial dependence of spin correlators is characteristic of an ordered ferrimagnetic chain with pseudospin moments of $\sigma = 1/2$ and $\tilde{S} = 3/2$.

A variation in the correlation functions under irradiation, when $n_{hv} \neq 0$, is demonstrated in Fig. 9. This figure presents the correlators $K_1(d)$ and $\langle h_f h_{f+d} \rangle$ for high intensity of irradiation ($n_{hv} = 0.5$). One can see that, in this limit, the functions $K_1(d)$ and $\langle h_f h_{f+d} \rangle$ take nonzero values only for odd d ; these values are $0.5\tilde{S}_2^2$ and $1/2$, respectively, where $\tilde{S}_2 = 2$ is the pseudospin moment of HS iron ions after irradiation. This behavior of correlators corresponds to an ordered set of isolated HS ions of iron in photoinduced spin states.

Figure 10 demonstrates the temperature dependence of the magnetic susceptibility of SCM-catena for three values of intensity of optical radiation: in the absence of radiation ($n_{hv} = 0$), under radiation of moderate intensity ($n_{hv} = 0.1$), and under superstrong radiation ($n_{hv} = 0.5$). One can see that, within the model formulated, the variation of the concentration of iron ions taking part in MMCT processes within a rather narrow range of $0 < n_{hv} < 10\%$ may lead to a significant modification of the temperature dependence of the magnetic susceptibility of the compound, changing the characteristic peak of this function by a factor of from 2 to 3.

8. CONCLUSIONS

By an example of an organic four-sublattice one-dimensional magnet catena- $[\text{Fe}^{\text{II}}(\text{ClO}_4)_2\{\text{Fe}^{\text{III}}(\text{bpca})_2\}]\text{ClO}_4$ (SCM-catena) with alternating HS and LS iron ions and with a mutually orthogonal orientation of easy-magnetization planes of nearest neighbor HS ions of iron, we have developed a quantum theory of anisotropic multisublattice magnets. The importance of the investigation of the spectral properties of this one-dimensional magnet among a large variety of single-chain magnets [6, 7] is associated with the necessity to establish an Ising-type character of the spectrum of elementary excitations and to determine whether the thermodynamic properties of SCM-catena can be described on the basis of the effective Ising model [30]. In this case, on the basis of the known redistribution of valence states of iron ions under irradiation, we had to quantitatively describe the experimentally observed variation in the magnetic susceptibility of SCM-catena.

The theoretical analysis of the quantum properties of multisublattice anisotropic magnets has been carried out by the diagram technique for Hubbard operators [32], which allows one to correctly describe systems with arbitrary nonequidistance of the energy spectrum of single-ion states. The latter fact is of special importance, because the characteristic energy of single-ion anisotropy in the materials analyzed is comparable with the energy of exchange interaction. As is known, quantum fluctuations play a significant role under these conditions, and the effects of single-ion anisotropy cannot be described on the phenomenological level.

The method developed has allowed us to investigate low-temperature properties of SCM-catena in the spin-wave approximation. Quantum fluctuations have been calculated with regard to renormalizations of the occupation numbers of HS states of iron ions. We have shown that, for these states, quantum fluctuations rather strongly renormalize the mean value of the modulus of the projection of the spin moment, $|\langle S^z \rangle|$, reducing it from the nominal value $S = 2$ to a value of $S \approx 3/2$ (the effect of quantum reduction of spin).

The spectral characteristics of SCM-catena obtained within the theory developed have allowed us to validate the experimentally observed analogy between low-temperature magnetic properties of this compound and similar properties of easy-axis, or even an Ising, magnet [30]. The calculation of the low-temperature spectral properties of the compound has shown that the excitation spectrum of SCM-catena is close to the excitation spectrum of the effective model of easy-axis magnet in which the parameter of easy-axis single-ion anisotropy is comparable with the exchange interaction constant. Moreover, it turns out that the excitation spectrum of both models is characterized by the presence of a gap of width much greater than the width of the spin-wave band. These facts

imply that the thermodynamic properties of the compound can be described in a wide temperature interval on the basis of the effective Ising model with pseudo-spin moments of $\tilde{S} = 3/2$ and $\sigma = 1/2$.

The possibility of transition to the Ising-type model has been demonstrated by comparing exact numerical calculations of the temperature dependence of the magnetization of chains of finite length for the original Heisenberg model and for the effective Ising model. Further analysis of the magnetic properties of the effective Ising model has been carried out with the use of the transfer-matrix technique. This has allowed us to carry out accurate calculations of both the thermodynamic means and the correlation functions of the system. The defects that arise at technological level and efficiently break the chain have been taken into account by introducing an ensemble of chains of finite length the average number of magnetic centers in which obeys the Poisson statistics.

The generalization of such an approach to the case when magnetic processes associated with photoinduced processes of electron transfer from one magnetically active ion to another arise in the system has allowed us to describe the magnetic properties of the compound in the presence of external optical irradiation. In particular, we have reproduced the experimentally observed modification of the temperature dependence of the magnetic susceptibility of SCM-catenas under irradiation [27]. A key point in this description is the introduction of an additional, special statistical ensemble of Ising chains each site of which can be occupied by iron ions in both original and photoinduced spin states. To obtain a correct alternation of iron ions in different spin states, we have introduced effective Coulomb-repulsion-type non-magnetic interactions. The application of the transfer-matrix method to such a statistical ensemble has allowed us to calculate various correlation functions of the system and trace the modification of the magnetic structure of the compound under irradiation.

Note also that the method developed in this work is not restricted to the compound considered; it can be applied to the description of experimentally observed modification of the temperature dependence of magnetic susceptibility under irradiation in other single-chain magnets as well [8, 25, 26].

APPENDIX A

The nonzero transverse and longitudinal parameters of representation, $\gamma_{\parallel}(p, q) = \gamma_{\parallel}^*(q, p) = \langle \psi_p | S^z | \psi_q \rangle$, $\Gamma_{\parallel}(p) = \langle \psi_p | S^z | \psi_p \rangle$, $\gamma_{\perp}(p, q) = \langle \psi_p | S^+ | \psi_q \rangle$, and $\Gamma_{\perp}(p) = \langle \psi_p | S^+ | \psi_p \rangle$, for iron ions in HS states are expressed as

$$\begin{aligned}
 \gamma_{\perp}(1, 2) &= 2 \cos \alpha \cos |\beta| \cos |\Omega| + \sqrt{6} e^{i(v-\kappa)} \sin |\beta| \sin |\Omega|, \\
 \gamma_{\perp}(2, 1) &= 2 e^{i\kappa} \sin \alpha \cos |\beta| \cos |\Omega| + \sqrt{6} e^{-iv} \sin |\beta| \cos |\Omega|, \\
 \gamma_{\perp}(1, 4) &= -2 e^{-i\kappa} \cos \alpha \cos |\beta| \sin |\Omega| + \sqrt{6} e^{iv} \sin |\beta| \cos |\Omega|, \\
 \gamma_{\perp}(4, 1) &= 2 \sin \alpha \cos |\beta| \cos |\Omega| - \sqrt{6} e^{-i(v-\kappa)} \sin |\beta| \sin |\Omega|, \\
 \gamma_{\perp}(2, 3) &= -2 (e^{i(v+\kappa)} \sin \alpha \sin |\beta| \cos |\gamma| \\
 &\quad - e^{-i(\delta-\kappa)} \cos \alpha \sin |\gamma|) \sin |\Omega| \\
 &\quad + \sqrt{6} \cos |\beta| \cos |\gamma| \cos \Omega, \\
 \gamma_{\perp}(3, 2) &= -2 (e^{-iv} \cos \alpha \sin |\beta| \cos |\gamma| \\
 &\quad + e^{i\delta} \sin \alpha \sin |\gamma|) \cos |\Omega| \\
 &\quad + \sqrt{6} e^{-i\kappa} \cos |\beta| \cos |\gamma| \sin \Omega, \\
 \gamma_{\perp}(2, 5) &= 2 (e^{i(\delta+v-\kappa)} \sin \alpha \sin |\beta| \sin |\gamma| \\
 &\quad + e^{-i\kappa} \cos \alpha \cos |\gamma|) \sin |\Omega| \\
 &\quad - \sqrt{6} \cos |\beta| \sin |\gamma| \cos \Omega, \\
 \gamma_{\perp}(5, 2) &= 2 (e^{i(\delta+v)} \cos \alpha \sin |\beta| \sin |\gamma| \\
 &\quad + \sin \alpha \cos |\gamma|) \cos |\Omega| \\
 &\quad - \sqrt{6} e^{i(\delta+\kappa)} \cos |\beta| \sin |\gamma| \sin \Omega, \\
 \gamma_{\perp}(3, 4) &= 2 (e^{-i(v+\kappa)} \cos \alpha \sin |\beta| \cos |\gamma| \\
 &\quad + e^{i(\delta-\kappa)} \sin \alpha \sin |\gamma|) \sin |\Omega| \\
 &\quad + \sqrt{6} \cos |\beta| \cos |\gamma| \cos \Omega, \\
 \gamma_{\perp}(4, 3) &= -2 (e^{iv} \sin \alpha \sin |\beta| \cos |\gamma| \\
 &\quad - e^{-i\delta} \cos \alpha \sin |\gamma|) \cos |\Omega| \\
 &\quad - \sqrt{6} e^{i\kappa} \cos |\beta| \cos |\gamma| \sin \Omega, \\
 \gamma_{\perp}(4, 5) &= 2 (e^{i(\delta+v)} \sin \alpha \sin |\beta| \sin |\gamma| \\
 &\quad + \cos \alpha \cos |\gamma|) \cos |\Omega| \\
 &\quad + \sqrt{6} e^{i(\delta+\kappa)} \cos |\beta| \sin |\gamma| \sin \Omega, \\
 \gamma_{\perp}(5, 4) &= -2 (e^{-i(\delta+v+\kappa)} \cos \alpha \sin |\beta| \sin |\gamma| \\
 &\quad - e^{-i\kappa} \sin \alpha \cos |\gamma|) \sin |\Omega| \\
 &\quad - \sqrt{6} e^{i\delta} \cos |\beta| \sin |\gamma| \cos \Omega, \\
 \gamma_{\parallel}(1, 3) &= -e^{-iv} \cos 2\alpha \sin 2\beta \cos \gamma \\
 &\quad - 2 e^{-i\delta} \sin 2\alpha \cos \beta \sin \gamma, \\
 \gamma_{\parallel}(1, 5) &= e^{-i(\delta+v)} \cos 2\alpha \sin 2\beta \cos \gamma \\
 &\quad - 2 \sin 2\alpha \cos \beta \cos \gamma, \\
 \gamma_{\parallel}(3, 5) &= -e^{i\delta} \cos 2\alpha (1 + \sin^2 \beta) \sin 2\gamma \\
 &\quad + 2 e^{i\delta} \sin 2\alpha \sin \beta [e^{-i(v+\delta)} \cos^2 \gamma - e^{i(v+\delta)} \sin^2 \gamma], \\
 \gamma_{\parallel}(2, 4) &= -\cos \kappa \sin 2\Omega, \\
 \Gamma_{\parallel}(1, 1) &= 2 \cos 2\alpha \cos^2 \beta,
 \end{aligned}$$

$$\Gamma_{\parallel}(2, 2) = \cos 2\Omega,$$

$$\Gamma_{\parallel}(4, 4) = -\cos 2\Omega,$$

$$\Gamma_{\parallel}(3, 3) = 2 \cos 2\alpha (\sin^2 \beta \cos^2 \gamma - \sin^2 \gamma),$$

$$\Gamma_{\parallel}(5, 5) = 2 \cos 2\alpha (\sin^2 \beta \sin^2 \gamma - \cos^2 \gamma) \\ - 2 \cos(\nu + \delta) \sin 2\alpha \sin \beta \sin 2\gamma.$$

APPENDIX B

$$\begin{aligned} \tilde{M}_{12}(q, \omega) = & -8 \left(\frac{J}{2}\right)^7 z_B^2(\omega) z_B^2(-\omega) (z_A(\omega) w(\omega) \\ & - z_A^2(\omega) z_A^2(-\omega)) \cos^4(2q) \\ & + 4 \left(\frac{J}{2}\right)^5 z_B(\omega) z_B(-\omega) (z_B(-\omega) w^2(\omega) \\ & - z_A^2(\omega) z_B(\omega) - 2z_A(\omega) z_A(-\omega) z_B(\omega)) \cos^2(2q) \\ & + \left(\frac{J}{2}\right)^3 (4z_A(\omega) z_B(\omega) z_B(-\omega) + 2z_A(-\omega) z_B^2(\omega) \\ & \times \cos^2(2q)) - \left(\frac{J}{2}\right) z_B(-\omega), \end{aligned} \quad (62)$$

$$\begin{aligned} \tilde{M}_{52}(q, \omega) = & -8 \left(\frac{J}{2}\right)^7 z_B^2(\omega) z_B^2(-\omega) w(\omega) \\ & \times (z_A(\omega) z_A(-\omega) - w_A(\omega)^2) \cos^4(2q) \\ & + 4 \left(\frac{J}{2}\right)^5 z_B(\omega) z_B(-\omega) w(\omega) (z_A(\omega) z_B(\omega), \\ & + z_A(-\omega) z_B(-\omega)) \cos^2(2q) \\ & - \left(\frac{J}{2}\right)^3 2z_B(\omega) z_B(-\omega) w(\omega) \cos^2(2q), \end{aligned} \quad (63)$$

$$\begin{aligned} \tilde{M}_{21}(q, \omega) = & 8 \left(\frac{J}{2}\right)^7 z_B(\omega) z_B(-\omega) (w^2(\omega) \\ & - z_A(\omega) z_A(-\omega))^2 \cos^4(2q) - \left(\frac{J}{2}\right) z_A(-\omega) \\ & + 4 \left(\frac{J}{2}\right)^5 z_B(\omega) (2z_A(\omega) z_B(\omega) + z_A(-\omega) z_B(-\omega)) \\ & \times (w^2(\omega) - z_A(\omega) z_A(-\omega)) \cos^2(2q) \\ & + \left(\frac{J}{2}\right)^3 [4z_A(\omega) z_A(-\omega) z_B(\omega) \\ & + 2(z_A^2(-\omega) z_B(-\omega) - w^2(\omega) z_B(\omega)) \cos^2(2q)], \end{aligned} \quad (64)$$

$$\begin{aligned} \tilde{M}_{61}(q, \omega) = & i \left(\frac{J}{2}\right)^3 (z_A(\omega) z_B(\omega) \\ & - z_A(-\omega) z_B(-\omega)) \sin(4q). \end{aligned} \quad (65)$$

ACKNOWLEDGMENTS

This work was supported by the Russian Foundation for Basic Research, project nos. 13-02-00523, 14-02-31237, and 15-42-04372.

REFERENCES

1. A. I. Smirnov and V. N. Glazkov, *J. Exp. Theor. Phys.* **105** (4), 861 (2007).
2. S.-L. Drechsler, O. Volkova, A. N. Vasiliev, N. Tristan, J. Richter, M. Schmitt, H. Rosner, J. Malek, R. Klingeler, A. A. Zvyagin, and B. Buchner, *Phys. Rev. Lett.* **98**, 077202 (2007).
3. L. E. Svistov, T. Fujita, H. Yamaguchi, S. Kimura, K. Omura, A. Prokofiev, A. I. Smirnov, Z. Honda, and M. Hagiwara, *JETP Lett.* **93** (1), 21 (2011).
4. L. A. Prozorova, S. S. Sosin, L. E. Svistov, N. Buttgen, J. B. Kemper, A. P. Reyes, S. Riggs, A. Prokofiev, and O. A. Petrenko, *Phys. Rev. B: Condens. Matter* **91**, 174410 (2015).
5. L. Bogani, A. Vindigni, R. Sessoli, and D. Gatteschi, *J. Mater. Chem.* **18**, 4750 (2008).
6. C. Coulon, H. Miyasaka, and R. Cl'eric, *Struct. Bonding (Berlin, Ger.)* **122**, 163 (2006).
7. W.-X. Zhang, R. Ishikawa, B. Breedlove, and M. Yamashita, *RSC Adv.* **3**, 3772 (2013).
8. T. Liu, H. Zheng, S. Kang, Y. Shiota, S. Hayami, M. Mito, O. Sato, K. Yoshizawa, S. Kanegawa, and C. Duan, *Nat. Commun.* **4**, 2826 (2013).
9. O. V. Billoni, V. Pianet, and D. A. Vindigni Pescia, *Phys. Rev. B: Condens. Matter* **84**, 064415 (2011).
10. R. Glauber, *J. Math. Phys.* **4**, 294 (1963).
11. L. Bogani, A. Caneschi, M. Fedi, D. Gatteschi, M. Massi, M. A. Novak, M. G. Pini, A. Rettori, R. Sessoli, and A. Vindigni, *Phys. Rev. Lett.* **92**, 207204 (2004).
12. C. Coulon, R. Cl'eric, L. Lecren, W. Wernsdorfer, and H. Miyasaka, *Phys. Rev. B: Condens. Matter* **69**, 132408 (2004).
13. A. Vindigni, L. Bogani, D. Gatteschi, R. Sessoli, A. Rettori, and M. A. Novak, *J. Magn. Magn. Mater.* **272–276**, 297 (2004).
14. Yu. B. Kudasov, *J. Exp. Theor. Phys.* **110** (2), 360 (2010).
15. M. G. Pini and A. Rettori, *Phys. Rev. B: Condens. Matter* **76**, 064407 (2007).
16. C. Coulon, R. Cl'eric, W. Wernsdorfer, T. Colin, A. Saitoh, N. Motokawa, and H. Miyasaka, *Phys. Rev. B: Condens. Matter* **76**, 214422 (2007).
17. A. Vindigni and M. G. Pini, *J. Phys.: Condens. Matter* **21**, 236007 (2009).
18. K. Bernot, J. Luzon, A. Caneschi, D. Gatteschi, R. Sessoli, L. Bogani, A. Vindigni, A. Rettori, and M. G. Pini, *Phys. Rev. B: Condens. Matter* **79**, 134419 (2009).
19. S. Sahoo, J.-P. Sutter, and S. Ramasesha, *J. Stat. Phys.* **147**, 181 (2012).
20. Yu. B. Kudasov, A. S. Korshunov, V. N. Pavlov, and D. A. Maslov, *Phys.—Usp.* **55** (12), 1169 (2012).
21. M. Nihei, T. Shiga, Y. Maeda, and H. Oshio, *Coord. Chem. Rev.* **251**, 2606 (2007).
22. P. Gamez, J. S. Costa, M. Quesada, and G. Aromi, *Dalton Trans.* **38**, 7845 (2009).
23. B. Weber and E.-G. Ja'ger, *Eur. J. Inorg. Chem.* **4**, 465 (2009).
24. M. A. Halcrow, *Chem. Soc. Rev.* **40**, 4119 (2011).

25. T. Liu, Y.-J. Zhang, S. Kanegawa, and O. Sato, *J. Am. Chem. Soc.* **132**, 8250 (2010).
26. N. Hoshino, F. Iijima, G. N. Newton, N. Yoshida, T. Shiga, H. Nojiri, A. Nakao, R. Kumai, Y. Murakami, and H. Oshio, *Nat. Chem.* **4** (11), 921 (2012).
27. M. Yamashita, T. Kajiwara, Yu. Kaneko, M. Nakano, Sh. Takaishi, T. Ito, H. Nojiri, N. Kojima, and M. Mito, *Presentation at Sixth International Symposium on Crystalline Organic Metals, Superconductors, and Ferromagnets* (2005).
28. E. Heintze, F. El Hallak, C. Clauß, A. Rettori, M. G. Pini, F. Totti, M. Dressel, and L. Bogani, *Nat. Mater.* **12**, 202 (2013).
29. T. Kajiwara, M. Nakano, Yu. Kaneko, Sh. Takaishi, T. Ito, M. Yamashita, A. Igashira-Kamiyama, H. Nojiri, Yu. Ono, and N. Kojima, *J. Am. Chem. Soc.* **127**, 10150 (2005).
30. T. Kajiwara, H. Tanaka, and M. Yamashita, *Pure Appl. Chem.* **80**, 2297 (2008).
31. T. Kajiwara, H. Tanaka, M. Nakano, Sh. Takaishi, Ya. Nakazawa, and M. Yamashita, *Inorg. Chem.* **49**, 8358 (2010).
32. R. O. Zaitsev, *Sov. Phys. JETP* **41** (1), 100 (1975).
33. V. V. Val'kov and T. A. Val'kova, *Sov. J. Low Temp. Phys.* **11** (9), 524 (1985).
34. V. V. Val'kov, T. A. Val'kova, and S. G. Ovchinnikov, *Sov. Phys. JETP* **61** (2), 323 (1985).
35. V. V. Val'kov and T. A. Val'kova, *Teor. Mat. Fiz.* **76** (1), 143 (1988).
36. V. I. Butrim, B. A. Ivanov, and Yu. A. Fridman, *Low Temp. Phys.* **38** (5), 395 (2012).
37. R. O. Zaitsev, *Diagrammatic Method in the Theory of Superconductivity and Ferromagnetism* (URSS, Moscow, 2004; URSS, Moscow, 2008).
38. V. V. Val'kov and S. G. Ovchinnikov, *Quasiparticles in Strongly Correlated Systems* (Siberian Branch of the Russian Academy of Sciences, Novosibirsk, 2001) [in Russian].
39. O. A. Kosmachev, Yu. A. Fridman, E. G. Galkina, and B. A. Ivanov, *J. Exp. Theor. Phys.* **120** (2), 281 (2015).
40. E. G. Galkina, V. I. Butrim, Yu. A. Fridman, B. A. Ivanov, and F. Nori, *Phys. Rev. B: Condens. Matter* **88**, 144420 (2013).
41. V. V. Val'kov, V. A. Mitskan, and G. A. Petrakovskii, *J. Exp. Theor. Phys.* **102** (2), 234 (2006).
42. V. V. Val'kov, S. V. Aksenov, and E. A. Ulanov, *J. Exp. Theor. Phys.* **119** (1), 124 (2014).
43. R. J. Baxter, *Exactly Solved Models in Statistical Mechanics* (Mir, Moscow, 1985; Academic Press, London, 2008).
44. L. Bogani, A. Caneschi, M. Fedi, D. Gatteschi, M. Massi, M. A. Novak, M. G. Pini, A. Rettori, R. Sessoli, and A. Vindigni, *Phys. Rev. Lett.* **92** (20–21), 207204 (2004).
45. F. A. Kassan-Ogly, *Phase Transitions* **722**, 223 (2000).
46. A. Vindigni, A. Rettori, M. G. Pini, C. Carbone, and P. Gambardella, *Appl. Phys. A* **82** (3), 385 (2006).
47. K. Bernot, J. Luzon, A. Caneschi, D. Gatteschi, R. Sessoli, L. Bogani, A. Vindigni, A. Rettori, and M. G. Pini, *Phys. Rev. B: Condens. Matter* **79** (13), 134419 (2009).
48. A. A. Lushnikov, *Sov. Phys. JETP* **29** (1), 120 (1968).
49. A. K. Arzhnikov and A. V. Vedyayev, *Sov. J. Low Temp. Phys.* **8**, 600 (1982).

Translated by I. Nikitin